eNeuro

Research Article: New Research | Development

The role of Even-skipped in Drosophila larval somatosensory circuit assembly

https://doi.org/10.1523/ENEURO.0403-21.2021

Cite as: eNeuro 2022; 10.1523/ENEURO.0403-21.2021

Received: 28 September 2021
Revised: 11 December 2021
Accepted: 19 December 2021

Title Page

Manuscript Title: The role of Even-skipped in Drosophila larval somatosensory circuit assembly

Abbreviated title: Eve in Drosophila ELs

Author names and affiliations, in order:

Zarion D. Marshall (1, 2), *Ellie S. Heckscher (1, 2)

Author contributions:

ESH and ZDM Designed research, Preformed research, Analyzed Data, Wrote the paper

*Corresponding author: heckscher@uchicago.edu

1) Department of Molecular Genetics and Cell Biology, University of Chicago, Chicago IL, 60637

2) Institute for Neuroscience University of Chicago, Chicago IL, 60637

Number of Tables 2; Number of Figures 10; Number of Multimedia 0

Number of words in Abstract 232, in Significance Statement117, in Introduction 647, in Discussion 1337

Conflict of interest statement: No

Acknowledgments: We would like to thank Chip Ferguson and Paschalis Kratsios (UChicago), Chris Doe (UOregon), and members of the Heckscher lab for comments that improved this manuscript. Also, thank you to Richard Baines (Manchester) for sharing Eve binding site data.

Funding sources: NIH grant R01-NS105748 University of Chicago, Department of Molecular Genetics and Cell Biology Start-up funds to ESH.

Abstract

Proper somatosensory circuit assembly is critical for processing somatosensory stimuli and for responding accordingly. In comparison to other sensory circuits (e.g., olfactory and visual), somatosensory circuits have unique anatomy and function. However, understanding of somatosensory circuit development lags far behind that of other sensory systems. For example, there are few identified transcription factors required for integration of interneurons into functional somatosensory circuits. Here, as a model, we examine one type of somatosensory interneuron, Even-skipped expressing Laterally placed interneurons (ELs) of the Drosophila larval nerve cord. Even-skipped (Eve) is a highly conserved, homeodomain transcription factor known to play a role in cell fate specification and neuronal axon guidance. Because marker genes are often functionally important in the cell types they define, we deleted *eve* specifically from EL interneurons. On the cell biological level, using single neuron labeling, we find *eve* plays several previously undescribed roles in refinement of neuron morphogenesis. Eve suppresses aberrant neurite branching, promotes axon elongation, and regulates dorsal-ventral dendrite position. On the circuit level, using optogenetics, calcium imaging, and behavioral analysis, we find *eve* is required in EL interneurons for the normal encoding of somatosensory stimuli and for normal mapping of outputs to behavior. We conclude that *eve* coordinately regulates multiple aspects of EL interneuron morphogenesis and is critically required to properly integrate EL interneurons into somatosensory circuits. Our data shed light on the genetic regulation of somatosensory circuit assembly.

Significance statement

In general, *even-skipped* (*eve*) genes are considered neural cell fate determinants. Here, we show that *eve* is required for refinement of axon and dendrite morphogenesis and for proper functional integration of neurons into somatosensory circuits. Thus, *eve* coordinately regulates multiple terminal neuronal features of a class of Eve-expressing interneurons, raising the possibility that, in other neuronal contexts, *eve* genes regulate a similar suite of features. Our study pushes the understanding of *eve* beyond the level of neuron morphology to the levels of circuit physiology and whole animal behavior. It thereby provides an updated understanding of *eve* in development. Further, our data identify *eve* as a genetic entry point for future study of sensorimotor circuit assembly in Drosophila.

Introduction (647/650 words)

Proper assembly of somatosensory circuits is critical for perception and movement (*Zeilig et al., 2012*). During somatosensory circuit development, interneurons wire up in precise patterns both with sensory neurons and with other CNS neurons (*Kohsaka et al., 2017; Clark et al., 2018; D'Elia and Dasen, 2018*). This is a multistep process involving, first, cell fate specification; then, axon outgrowth and dendrite morphogenesis; and finally, functional integration of neuronal inputs and outputs into the circuit. However, in comparison to other sensory systems (e.g., visual and olfactory), the assembly of the somatosensory system is still poorly understood (*Meng and Heckscher, 2021*).

The Drosophila larval nerve cord is an excellent system to study somatosensory circuit development. The organization of Drosophila and vertebrate somatosensory circuits is similar. For example, in both, a diversity of sensory neurons project axons to distinct dorsal-ventral regions (or laminae) in the CNS (*Zlatic et al., 2009; Rexed 1952*). Genetically-defined subtypes of somatosensory interneurons synapse with specific sensory neurons, and those interneurons contribute to either local reflex circuits or send information to the brain (*Lai et al., 2016; Wreden et al., 2017; Heckscher et al., 2015*). Therefore, principles uncovered in studies of Drosophila have the potential to be broadly relevant to vertebrate somatosensory circuit development.

In Drosophila, several aspects of somatosensory circuit development are well understood. In the PNS, specific transcription factors that regulate sensory neuron dendrite morphogenesis have been identified (*Zlatic et al., 2003; Hattori et al., 2007; Parrish et al., 2006*). In the CNS, early cell fate specification and the transcriptional regulation of axon guidance have been characterized (*Santiago et al., 2014; Stratmann et al., 2019*). However, most studies of neurons

in the Drosophila CNS have focused on experimentally accessible motor neurons. Motor neurons are fundamentally distinct from somatosensory interneurons. Axons of motor neurons exit the CNS, and in general, dendrites of motor neurons do not get direct synaptic input from sensory neurons (*Couton et al., 2015*). In Drosophila, there remain large gaps in our understanding of the genetic control of somatosensory interneuron morphogenesis, specifically in control of dendrite morphology and circuit integration. Furthermore, it is unclear to what extent multiple terminal features, such as axon and dendrite morphology, are coordinately controlled by single transcription factors (*Kurmangaliyev et al., 2019*).

In this study, as a model, we focus on Drosophila larval EL interneurons. ELs are named for their expression of the transcription factor, Even-skipped (Eve) and their Lateral cell body position. EL interneurons all process somatosensory stimuli and are necessary for normal behavior (*Heckscher et al., 2015)*. We focus on ELs because in comparison to other Drosophila somatosensory interneurons, the developmental origins of ELs are known, and reagents to label ELs in embryos and larvae are available *(Fujioka et al., 1999*). To study the transcriptional control of EL development, we took a candidate gene approach focusing on the role of *eve*. *eve* encodes a conserved homeobox transcription factor. *eve* or its homologs are expressed in neurons in animals across phyla (*Ferrier et al., 2001; Heckscher et al., 2015).* We reasoned that *eve* is likely to play an important role in ELs because cell type specific transcription factor genes often are important in the cell types they define. Further, in general, *eve* and its homologs play roles in cell fate specification and axon guidance (*Doe 1998; Landgraf et al., 1999; Moran-Rivard et al., 2001; Esmaeii et al., 2002; Fujioka et al., 2003; Pym et al., 2006; Zarin et al., 2014; Juarez-Morales et al., 2016*). Here, we show *eve* is required for multiple aspects of terminal neuronal development and for proper functional integration of ELs into sensorimotor circuits. Specifically,

99 *eve* regulates neurite branching, axon extension, dendrite positioning, formation of functional
100 inputs, and mapping of functional outputs, as well as whole animal behavior. Thus, we uncover
101 several, previously undescribed roles for *eve* in neuronal physiology, and we identify *eve* as a
102 transcriptional regulator of Drosophila somatosensory circuit assembly.

Materials and Methods (1276/3000 words)

Fly Genetics

Standard methods were used to propagate fly stocks. Unless otherwise noted, larvae were raised at 25C and fed yeast paste containing water and yeast (5:3 ratio by weight). For optogenetics experiments, yeast paste containing 100uL all trans retinal (ATR) was used. For a list of stocks used in this study see Table 1.

Species sex

In these experiments, embryos and early stage larvae were used. At these developmental stages, flies have no distinguishing sexual characteristics. So all experiments were conducted in a manner that was blind to sex.

Immunostaining

We used standard methods (*Meng et al., 2019; Meng et al., 2020*). Larval brains were pulled at ambient temperature within a seven-minute window. Brains were fixed in freshly prepared 1x phosphate buffered saline containing 4% formaldehyde for seven to ten minutes. Many primary antibodies were obtained from Developmental Studies Hybridoma Bank, created by the NICHD of the NIH and maintained at The University of Iowa, Department of Biology. See Table 1 for primary antibodies. Secondary antibodies were from Jackson ImmunoResearch (West Grove, PA) and were used according to manufacturer's instructions. Images were acquired on a Zeiss 800 confocal microscope with 40X objective. Embryos were staged for imaging based on standard morphological criteria**.**

Four ways to label ELs interneurons

In this study, we use four ways to label ELs (*Table 2*): 1) *Eve antibody staining*. In wild type, anti-Eve labels motor neurons and EL interneurons. In EL eve mutants, anti-Eve staining is lost

from the ELs. Notably, in EL eve mutants in trans to a hypomorphic *eve* allele, *eve(5),* which generates a truncated Eve protein, anti-Eve can be used to track ELs. 2) *EL-GAL4*. In wild type, *EL-GAL4* expresses in ELs from the middle of embryogenesis until the middle of larval development. However, in EL eve mutants, *EL-GAL4* drives only a pulse of gene expression. Thus, in ELs, Eve is dispensable for initiation of *EL-GAL4* expression, but is required to maintain *EL-GAL4* expression. 3) *EL-GAL4 with a permanent labeling cassette.* To positively mark ELs in an EL eve mutant background using *EL-GAL4,* we added a FLP-based permanent labeling cassette (*UAS-FLP, actin-FRT-Stop-FRT-GAL4*). 4) *11F02-GAL4*. In wild type, *11F02-GAL4* drives expression in the late-born subset of ELs, as well as a few other uncharacterized neurons (*Heckscher et al., 2014)*. *11F02-GAL4* expression is unchanged in EL eve mutants.

Larval behavior

L1 larvae were collected from zero to six hours after hatching. All larvae were rinsed in mesh chambers under dH20 until they were freed from food debris. Collected larvae were placed on 5 mm thick 2% agarose gels set in 5.5 cm wide Petri dishes at least 15 minutes before recording. All recordings were done at 22^{o}C to 25^{o}C. Five to 30 larvae were allowed to freely crawl on a gel per recording. For pinching assay, pinches were delivered to the side of the larval body wall with a pair of forceps. A larva was considered to be rolling if the trachea disappeared under one side of the larva body and reappeared on the other side. Note that this criterion for a roll is not based on larval speed. For hunching assay, a vibration was delivered to the larvae using the speaker and sound described below. Hunches were considered to be a shortening of the distance between the head and body center associated with a pause in crawling, but not a head turn. For left-right asymmetry and crawling speed assays, larvae were recorded in our custom-built behavior rig (Wreden et al., 2017). Images were acquired at 10 frames per second. For optogenetic

149 experiments, all larvae were recorded 48 to 54 hours after hatching. Ten to 100 larvae were
150 placed on a rectangular 5 mm thick agarose gel at least 15min before recording. Recordings
151 began with a 30 second period of no stimulus followed by a 30 second period of stimulating light
152 and ending with a final 30 second period of no stimulus. For further setup details, please refer to
153 Wreden et al., 2017.

154 Larvae were tracked using FIMTracker (*Risse et al., 2017*) software using default
155 parameters including five spline points—this includes centroid, head, and tail points, plus two
156 other points, one halfway between head and centroid and one halfway between the tail and
157 centroid. Larvae were discarded from analysis if 1) the larva's track was less than 300 frames 2)
158 the larva was improperly masked or 3) if occasionally the larva collided with another larva and it
159 was not rectified by thresholding. Tracks were then analyzed using custom scripts (*Heckscher et*
160 *al., 2015*) on MATLAB (Mathworks). Speeds were calculated using the center spline point over
161 a 10 frame (1 second) window. Statistical tests were performed using Prism 9 software
162 (GraphPad).

163 **Calcium imaging**

164 For calcium imaging experiments, all larvae were within 6 hours of age on the day of recording
165 and collected 48 to 54 hours after hatching. Larvae expressing GCaMP6m (*UAS-FLP, act5C-*
166 *FRT.stop-GAL4; ΔEL, Df(2R)eve/+; EL-GAL4/UASGCaMP6m* or *UAS-FLP, act5C-FRT.stop-*
167 *GAL4; ΔEL, Df(2R)eve/ΔEL, Df(2R)eve; EL-GAL4/UAS-GCaMP6m*) were rinsed with water and
168 placed ventral side up on agarose pads with a 22 mm x 22 mm coverslip placed on top. Pads
169 were made by pouring 3% agarose into a well. Recordings began with a 30 second period of no
170 stimulus followed by a 30 second period of sound stimulus and ending with a final 30 second
171 period of no stimulus. A Visaton FR12, 4 Ohm speaker (5 inches diameter) and a PYLE PCA2

stereo power amplifier was used to project sound. For further details, refer to Wreden et al., 2017. Images were acquired on a Zeiss LSM 800 confocal microscope using 0.1%–0.2% 488 nm laser power with the pinhole entirely open. Images were acquired at 3 frames per second using a 10X (0.3 NA) or 20X (0.8 NA) objective. The calcium signal was continuously collected before, during, and after the stimulus. Extracting changes in GCaMP6m fluorescence amplitude was done using Fiji as in Wreden et al., 2017. A region of interest (ROI) that included the larval nerve cord was manually drawn, and the mean fluorescence within the ROI was calculated for each time point.

Single Neuron Labeling

We labeled single neurons using MultiColor FLP Out (MCFO, *Nern et al., 2015*). MCFO stochastically labels the membranes with epitopes in cells within a GAL4 pattern. MCFO uses FLP recombinase, which we also use to label larval EL neurons in EL eve mutants (Table 2). So, we cannot use these reagents together. Here, for MCFO, we used *11F02-GAL4,* which is expressed in late-born ELs and three poorly characterized non-EL interneurons directly adjacent to ELs (*Heckscher et al., 2014; Wreden et al., 2017*). For *11F02-GAL4* to be useful, we needed to distinguish between ELs and non-ELs in wild type and EL eve mutant backgrounds. In both backgrounds, we performed single neuron MCFO labeling. In both backgrounds, we can identify three non-EL neurons based on morphology, which we call: 11F02d, 11F02m, and 11F02z. We conclude that loss of Eve from ELs does not have gross non-autonomous effects on non-EL neurons. We also conclude that we can distinguish between EL and non-EL neurons in EL eve mutants. To obtain single cell clones, adult flies were allowed to lay eggs for 24 hours on apple juice caps. Caps were heat shocked in a water bath at 37C to 39C for 15 to 30 minutes and incubated at 25C for 4 to 5 hours. First instar larvae were dissected. Their brains were stained for

HA, Flag, and V5 epitopes to visualize single cell clones. Larvae were also stained for Eve protein to confirm the identity of each single cell clone as an EL, and to assign segmental identity to each clone. Clones were imaged on a Zeiss 880 or 800 confocal microscope. We generated more than 115 single-cell clones. Among these clones, we saw each neuronal morphology in a minimum of two independently-derived clones (i.e., larvae). Each clone was analyzed in dorsal and posterior views.

RESULTS (2,336 words)

In EL eve mutants, EL interneurons lack *eve* expression

The objective of this study was to determine the role of the transcription factor, Even-skipped (Eve) in EL somatosensory interneurons. *eve* is an essential gene in Drosophila. It is expressed in stripes in early embryos, in other developing tissues, as well as in a subset of motor neurons and EL interneurons (*Heckscher et al., 2014; Frasch, 1987; Figure 1A*). In this study, we removed *e* *eve* specifically from ELs using "EL eve mutants", which were previously generated by Fujioka and colleagues *(Fujioka et al., 2003*). Briefly, a genomic construct containing all *eve* regulatory elements was generated (*Figure 1C*). This construct rescues *eve* null mutants to viability, and *eve* is expressed at normal levels and in normal locations *(Fujioka et al., 2003*). Fujioka and colleagues deleted from the construct a regulatory region sufficient to drive *eve* expression in ELs, thereby making a "ΔEL" construct (*Figure 1C*; *Fujioka et al., 1999; Fujioka et al., 2003*). When *eve* null alleles are rescued with ΔEL, *eve* is expressed at normal levels and locations everywhere except ELs interneurons, which completely lack *eve* (*Figure 1B; Fujioka et al., 2003*).

***eve* regulates multiple aspects of interneuron morphogenesis**

eve or its homologs (e.g. *evx* genes) often regulate neuronal axonal pathfinding. For example, in mouse spinal cord, *evx1* is required for V0v interneurons to send axons across the midline (*Moran-Rivard et al., 2001*). In Drosophila or *C. elegans* motor neurons, loss of *eve* genes results in dramatic changes in axon trajectories (*Esmaeili et al., 2002; Fujioka et al., 2003*). In contrast, in Zebrafish, *evx1/2*(-) V0v interneurons have normal axonal morphology (*Juárez-Morales et al., 2016*). These data demonstrate that *eve* plays a context dependent role in axons and raise the

question to what extent *eve* regulates EL interneuron axon morphogenesis in Drosophila larvae.

In embryos, we characterized EL morphology by expressing a membrane localized GFP. In stage 15 embryos, in both control and EL eve mutants, EL axons cross the midline (*Figure 2A-C*). In stage 16 embryos, we additionally stained with anti-Fas2 to visualize three fascicles in the neuropile—lateral, intermediate, and medial (*Landgraf et al., 2003*). In control, after midline crossing, most ELs grow laterally until reaching the intermediate fascicle and extend toward the anterior. In a subset of segments, ELs extend to the anterior along both intermediate and medial fascicles *(Figure 2D, F*). In EL eve mutants, however, a larger proportion of ELs extend along both the intermediate and medial fascicles. Further, in some segments, ELs project along the intermediate and lateral fascicles, a phenotype never observed in controls (*Figure 2E, F)*. In stage 17 embryos (the final stage of embryogenesis), in control, ELs project so far to the anterior that they reach the next segment, making a ladder like pattern (*Figure 2G)*. In contrast, in EL eve mutants, only a small proportion of *eve*(-) ELs reach the next segment (*Figure 2H, I*).

At larval stages, ELs have mature morphologies and are incorporated into functioning somatosensory circuits. We labeled individual ELs, using MultiColor FLP Out*,* which allows us to determine which part of the EL—axon, dendrite, or both—is impacted by loss of *eve* (*Nern et al., 2015)*. We restricted our analysis to local, late-born ELs, because they were most abundantly labeled in our dataset (*Figure 3A*). First, we focused our analysis along medial-lateral and anterior-posterior axes because in Figure 2 we detected defects along these axes. We used Sholl analysis to count the number of intersections between an EL neurite and concentric circles with increasing radii (1µm intervals) centered on the soma (Sholl 1953). We plotted the median, minimum, and maximum number of intersections versus circle radius to generate a description of arborization. In control, local, late-born ELs have two sets of branching neurites off the main

neurite. Ipsilaterally (same side) dendritic neurites are found ~20 microns from the soma. Contralaterally (opposite side) axonal neurites branch ~50 microns from the soma (*Figure 3B, D*). In EL eve mutants, neurites of *eve*(-) ELs branched excessively off the main neurite near the soma and in the midline, which is never seen in wild type (*Figure 3C, arrowheads*). Furthermore, *eve*(-) EL axons are less extended, branching at ~40 microns from the soma (*Figure 3C, arrow*). These changes are reflected in a statistically significant difference in the distribution of intersections (*Figure 3F*).

Next, in the same set of larval clones as shown in Figure 3, we characterized ELs along the dorsal-ventral axis. For somatosensory interneuron dendrites, positioning along the dorsal-ventral axis is particularly important because different sensory neurons axons project to different dorsal-ventral domains within the CNS *(Landgraf et al., 2003).* Therefore, dorsal-ventral positioning of somatosensory interneuron dendrites is expected to dictate the types of sensory input received by a given interneuron. Currently, the molecular control of dorsal-ventral dendrite positioning of somatosensory interneurons is extremely poorly understood. Here, we counted the number of dorsally and ventrally projecting ipsilateral branches (i.e., dendrite). In control, nearly all *eve*(+) ELs have dorsally, but not ventrally, projecting dendrites (*Figure 4A, C-D*). In EL eve mutants, there is a significant reduction in dorsally projecting dendrites and a significant increase in ventrally projecting dendrites for *eve*(-) ELs (*Figure 4B, C-D)*.

Finally, we asked if loss of *eve* transforms the ELs into another interneuron type. To do so, we took both anatomical and genetic approaches. Anatomically, we mined the Drosophila larval connectome (*Ohyama et al., 2015*). We looked at each local neuron in the first abdominal segment, but found no neurons with morphology matching that of *eve*(-) EL interneurons. Genetically, we looked for large-scale changes in gene expression, which often accompany cell

fate changes. We surveyed 19 genes that were candidates to be regulated by *eve* in ELs. These candidates included genes regulated by *eve* in non-EL cell types (En, FasII, HB9, Islet, see Figure 5A-B), genes expressed in ELs (Castor, Eagle, Zfh2, Knot, Kruppel, Nab, Pdm2, Seven-up, see Figure 5C-D), and genes with putative Eve binding sites (Antp, AbdA/Ubx, AbdB, Cut, Dpn, Repo) (*Pym et al., 2006*;*; Broihier and Skeath, 2002*). There are no obvious changes in expression for any of these genes in *eve*(-) ELs. Taken together, these data support the conclusion that, in ELs, Eve is not repressing alternative interneuron fate.

In summary, we find that, in ELs*, eve* is not required for the initial step of EL morphogenesis—axon midline crossing. However, *eve* is required for later stages of EL morphogenesis, refining morphology in all three axes—medial-lateral, anterior-posterior, and dorsal-ventral. Further, *eve* is required in both axons and dendrites. Thus, in EL interneurons, *eve* coordinately regulates multiple aspects of morphogenesis. Finally, we find no evidence to support the idea that, in ELs, Eve represses alternative neuronal fates because *eve*(-) EL interneurons do not resemble any other wild type interneuron.

Loss of *eve* disrupts EL somatosensory stimulus encoding

In wild type animals, EL interneurons encode somatosensory stimuli. Late-born ELs get direct synaptic input from proprioceptive sensory neurons and indirect proprioceptive input via Jaam interneurons (*Figure 6A; Heckscher et al., 2015).* Early-born ELs get direct synaptic input from vibration sensitive (chordotonal) sensory neurons and indirect chordotonal input via Basin interneurons (*Figure 6B*; *Wreden et al., 2017).* The observation that *eve*(-) EL dendrites are mispositioned raised the possibility that *eve* is required for ELs to properly encode somatosensory stimuli (*Figure 4*). We test this idea here.

Mispositioned dendrites in eve(-) EL interneurons likely disrupt the ability of ELs to form connections with their normal sensory neuron input partners (*Figure 5C, E*). Alternatively, ELs could still form synapses with input partners via a compensatory mechanism (*Figure 6F*). It is essential to consider this alternative because a recent study revealed the existence of compensatory mechanisms in Drosophila sensory neuron-to-somatosensory interneuron wiring (*Valdes-Aleman et al., 2021)*. Specifically, genetically mispositioned sensory neurons form synapses with many of their normal interneuron partners, which grow abnormally to reach the mispositioned sensory neurons *(Figure 6D*). In control and EL eve mutants, we characterized the position of sensory neurons by labeling vibration and proprioceptive sensory neurons with *iav-GAL4* and *0165-GAL4* driving membrane GFP, but find no differences in sensory neuron axon position (*Figure 6G-H*).

Next, we tested the idea that *eve* is required for normal EL somatosensory stimulus encoding. Drosophila larvae are optically clear so we used calcium signals in intact larvae to monitor EL activity. Specifically, a larva expressing GCaMP6m in ELs was placed on a bed of agarose with a coverslip on top *(Figure 7A*). In this preparation, larvae do not crawl, but they move, which stimulates proprioceptors, and sound can be used to stimulate vibration-sensitive chordotonal sensory neurons (*Wreden et al., 2017).* In a single recording, we imaged baseline EL fluorescence, EL activity while the sound is played, and return to baseline. In control, there are small amplitude changes in fluorescence intensity in ELs during periods of self-movement and large amplitude changes in response to vibration (*Figure 6B, D*). In EL eve mutants, there is only bleaching of the calcium signal (*Figure 7C, E*).

We conclude that in the absence of *eve*, EL interneurons no longer normally encode somatosensory stimuli.

316

317 **Upon loss of *eve*, EL outputs are anatomically and functionally reconfigured**

318 EL interneurons are necessary for normal Drosophila larval behavior (*Heckscher et al., 2015)*.
319 Late-born ELs contribute to a circuit that regulates left-right symmetrical crawling, and early-
320 born ELs contribute to a circuit that triggers fast escape rolling (*Wreden et al., 2017).* The
321 observation that *eve*(-) EL axons are less extended raised the possibility that EL output circuits
322 could be reconfigured (*Figure 3*).

323 The specific output partners of EL interneurons are not well characterized, and so we
324 determined the location of *eve*(-) EL output synapses. In control and EL eve mutants, we
325 visualized presynaptic nerve termini, using expression of a V5 epitope tagged Brunchpilot (BRP-
326 V5) protein (*Wagh et al., 2006; Chen et al., 2013*). In control, BRP signal is concentrated in
327 large puncta in the central intermediate and medial region of the neuropile (*Figure 8A'*).
328 However, in EL eve mutants, BRP signal is found diffusely throughout the neuropile (*Figure*
329 *8B'*). To quantify this, we used Fas2 expression to subdivide the neuropile into medial (M),
330 intermediate (I), and lateral (L) zones, and scored for BRP signal in each zone (*Figure 8C-D*).
331 We find a significant increase in lateral signal in EL eve mutants compared to control. These
332 data suggest that *eve*(-) EL interneurons output synapses are relocated.

333 We used functional approaches to determine the extent to which relocation of *eve*(-) EL
334 output synapses change circuit function. We recorded spontaneously occurring crawling in
335 control and in EL eve mutant larvae (*Figure 9*). We calculated crawling speed as centroid
336 position over time and left-right body symmetry using the angles between centroid and head
337 position and centroid and tail position. EL eve mutants crawl significantly slower than control
338 (*Figure 9A-C)* with left-right asymmetrical body posture (*Figure 9D, F-H*). We had previously

recorded the behavior of larvae that entirely lack EL interneurons, and here we noticed that, in comparison, EL eve mutant larvae have more severe crawling defects (*Heckscher et al., 2017*). This is quantified as significantly greater left-right asymmetry in larvae with *eve*(-) ELs than in larvae without ELs (*Figure 9D-H).* The discrepancy between severity of the phenotypes could be explained by the idea that mispositioned *eve*(-) EL output synapses make new, functional connections, which could provide a dominant negative effect at the circuit level (see Discussion).

The crawling defects provide strong functional evidence that *eve* is required in EL interneurons for normal somatosensory circuit function (*Figure 9*). However, we demonstrated that in *eve*(-) ELs sensory encoding is disrupted (*Figure 7*). Therefore, it is possible that dysfunction in sensory encoding could explain the observed behavioral deficits. And so, we assayed the behavioral response to optogenetic stimulation of *eve*(-) ELs . Optogenetics uses light to activate neurons and bypasses the need for any input from upstream neurons. We reasoned that optogenetic stimulation of eve(-) ELs might elicit a novel behavior, consistent with the idea that eve(-) EL output synapses are remapped. In control and EL eve mutants, we expressed the optogenetic effector, CsChrimson, and fed larvae all trans retinal (ATR), a cofactor needed for CsChrimson light sensitivity. As expected, in response to light, any larva not fed ATR fails to respond (*Figure 10D, E*). Also, as expected, control larvae fed ATR roll upon light exposure, which is quantified as fast centroid movement over time (*Figure 10A, D, F*). In EL eve mutants fed ATR, in response to light, larvae preform a novel behavior—a dorsal body bend. This is quantified as a small increase in centroid movement over time (*Figure 10B, E*, *G*). The body bend is an extreme C shape where the head and tail nearly touch, and to our knowledge, does not occur naturally in *Drosophila melanogaster*. Dorsal bending is robust, displayed by nearly every EL eve mutant larva. This demonstrates that *eve*(-) EL output synapses are

functional and that their activation leads to a novel behavior.

Activation of eve(-) EL interneurons could lead to novel behavior for two reasons. First, EL output synapses could be re mapped to new, downstream targets and away from roll inducing circuits. Alternatively, circuits mediating rolling and other sensorimotor transformations could be generally dysfunctional. This possibility needed to be tested because homeodomain proteins, including Eve, can have non-autonomous effects (*Lee et al., 2019*). To probe the function of rolling circuits, we provided a body wall pinch, which served as a mechanical and noxious stimulus, to both control and EL eve mutants *(Hwang et al., 2007*). In both genotypes, larvae roll in response to pinch (*Figure 10H*). Thus, in EL eve mutant larvae, roll inducing circuits are not disrupted. Further, we found that both EL eve mutant and control larvae respond to vibration with a hunch (*Figure 10I*). Thus, in EL eve mutant larvae, somatosensory stimuli can be perceived and transformed into appropriate motor output, and somatosensory circuits are not generally dysfunctional. We conclude that, in *eve*(-) ELs, output synapses are no longer mapped to roll inducing circuits, but instead to novel targets.

Discussion

In this study, we removed the conserved, homeodomain transcription factor, Even-skipped (Eve), from Drosophila Even-skipped-expressing Lateral placed interneurons (ELs, *Figure 1*). We found that *eve* regulates multiple aspects of EL interneuon morphogenesis (*Figures 2-4*), and that *eve* is required for the proper integration of ELs into somatosensory circuits at both the input (*Figures 6-7*) and output (*Figures 8-10*) levels.

Previously undescribed roles for *eve* in neuronal morphogenesis

Here, we show that *eve* is required for positioning EL interneuron neurites in all three axes (i.e., medial-lateral, anterior-posterior, and dorsal-ventral) (*Figures 2-4*). In Drosophila, each axis is patterned by a separate ligand/receptor signaling system (*Zlatic et al. 2009; Evans and Bashaw, 2009; Emerson et al., 2013*). But, how individual interneurons read and interpret each signal is not well-understood. Our data suggest *eve* is important for ELs to simultaneously read and/or interpret multiple ligand gradients simultaneously.

Generally, *eve* is considered a cell fate determinant. For example, in mouse V0v interneurons, *evx1* represses expression of *en1,* a marker of V1 interneuron identities (*Moran-Rivard et al, 2001*). In V0v interneurons that lack *evx1*, *en1* expression is derepressed and take on V1-like axonal projections. Similar fate changes are seen in Drosophila and *C. elegans* motor neurons when *eve* is disrupted (*Landgraf et al., 1999; Esmaeili* et al., 2002). Our data are more consistent with the idea that *eve* plays a role in the refinement of EL morphogenesis. In support for the morphogenetic refinement model is, first, in wild type, there are no neurons with morphology that matches the morphology of *eve*(-) ELs, as would be expected by a cell fate switching model. Second, there are no obvious large-scale changes in gene expression, which are

typically associated with cell fate changes (*Figure 5*). Third, *eve* in ELs is not playing a role in initial morphogenesis (see next paragraph for more).

Both *eve*(-) and eve(+) ELs cross the midline at embryonic stage 15 (*Figures 2A-C*). Thus, *eve* is either dispensable for initial morphogenesis, or in EL eve mutants there is an undetectable pulse of early *eve* expression in ELs. But, we and others have not found Eve protein expression in ELs in EL eve mutants at any stage of development (*Figure 1A-B, Fujioka et al., 2003).* In later stage embryos and larvae, we observe morphological defects in *eve*(-) ELs (*Figures 2D-H, Figure 3, and Figure 4*). This raises the possibility that, in general, *eve* genes may play a later role in morphogenesis. This is consistent with the observation that, in mouse V0v interneurons, there is early *evx1* expression and later *evx2* expression. However, the later role of *evx2* is unknown (*Moran-Rivard et al., 2001).*

In general, *eve* genes are known to regulate axon morphogenesis (*Doe 1998; Landgraf et al., 1999; Moran-Rivard et al., 2001; Esmaeii et al., 2002; Fujioka et al., 2003*). In this study, we show that late-born *eve*(-) ELs have axonal defects (*Figures 3-4)*. Notably, the role of *eve* in dendrite morphogenesis is extremely poorly characterized. The distinction between dendrite and axon is important because these two compartments carry out different functions. Further, in Drosophila, interneuron axons and dendrites are structurally different. Dendrites are often highly branched, and lack mitochondria and post-synaptic machinery. Whereas, axon terminals (boutons) are full of mitochondria, pools of synaptic vesicles, microtubules, and vesicle release sites. Each part of the arbor (axon or dendrite) can be independently controlled by different transcription factors (*Kurmangaliyev et al., 2019*). For example, in Drosophila sensory neurons, the transcription factors Knot and Cut specifically regulate dendrite morphogenesis, but not axonal morphology (*Jinushi-Nakao et al., 2007*). Thus, in Drosophila, axon and dendrite

morphology can be controlled as independent modules. Here, we show that in addition to regulating axon morphology, *eve* regulates dorsal-ventral dendrite positioning (*Figure 4*). *eve* is also required for dendrite morphogenesis in RP motor neurons (Fujioka et al. 2003). Taken together our data show that *eve* coordinately regulates multiple aspects of neuronal morphogenesis, and that coordinate control may be a widely-occurring role for neuronal *eve*.

even-skipped in ELs plays a role in somatosensory circuit assembly

Neuronal circuits are functional units of the nervous system. Sensorimotor circuits, specifically, transform somatosensory stimuli into motor output. Therefore, functional assays are required for the study of somatosensory circuit assembly. However, because the circuit context of individual interneurons is not well-characterized, often researchers rely on anatomical assays to infer changes at the circuit level. One reason an anatomical approach can be flawed is the existence of compensatory mechanisms that allow for relatively normal circuit wiring despite changes in neuron morphology (*Valdes-Aleman et al., 2021; Landgraf et al. 1999; Meng and Heckscher, 2021*). In this study, we link defects in neuronal morphology to changes in circuit function, thereby explicitly demonstrating the role of *eve* in somatosensory circuit assembly.

The role of eve *in formation of functional input synapses.* We show that *eve* is required for somatosensory stimulus encoding by ELs (*Figure 7*). Based on known connectivity of ELs with other neurons (*Figure 6A*), we infer that in ELs, *eve* is required for the formation of at least four types of functional input synapses: those from vibration (chordotonal) sensory neurons to early-born ELs, from vibration-sensitive interneurons (Basins) to early-born ELs, from proprioceptive sensory neurons to late-born ELs, and from proprioceptive-sensitive interneurons (Jaams) to late-born ELs. The likely cell biological underpinning, at least for late-born ELs, is

445 that axons from input sensory neurons (*Figure 6G-H*) are not in close enough proximity to make
446 synaptic contact with *eve*(-) ELs (*Figure 4)*. Due to technical limitations, we could not visualize
447 dendrite morphology of early-born ELs.

448 In the Drosophila nerve cord, there is unidirectional compensatory growth from
449 interneurons to genetically misplaced sensory neurons (*Valdes-Aleman et al., 2021*, *Figure 6C-*
450 *D*). Thus, Drosophila sensory neuron-to-interneuron wiring can be robust to morphological
451 alterations to circuit components. The observation (*Figure 6G-H*) that sensory neurons do not
452 grow to reach mispositioned *eve*(-) EL dendrites raises two possibilities: 1) In this system,
453 compensatory growth is unidirectional (i.e., interneurons grow to misplaced sensory neurons, but
454 not vice versa). 2) Alternatively, compensatory growth is bidirectional, however, *eve* is required
455 for this process. Future experiments will be needed to distinguish between these models.

456 *The role of* eve *positioning output synapses.* Our data show *eve*(-) EL output synapses are
457 functional, but remapped. Spontaneously-occurring crawling behavior is disrupted in EL eve
458 mutants (*Figure7*), and that this disruption is significantly worse than in larvae which lack EL
459 neurons altogether. This could be explained by requirement for ELs during early circuit
460 development (e.g., acting as a scaffold for normal axonal pathfinding for other neurons).
461 Alternatively, mature *eve*(-) ELs could exert a dominant negative effect at the level of circuit
462 function. We favor the latter idea because it is consistent with the optogenetic experiments
463 presented in Figure 9, and the anatomical data presented in Figure 7. Figure 7 shows that in
464 Controls, EL output synapses are excluded from many zones of the neuropile including the
465 dorsal lateral zone, which houses the dendrites of dorsally-projecting motor neurons. However,
466 *eve*(-) ELs are likely to form output synapses in this region. This specific re-distribution of
467 output synapses is notable because it raises the possibility that *eve*(-) ELs output synapses (ELs

468 are excitatory) could be directly re-mapped to dorsal motor neurons. Such a re-mapping could
469 explain the novel behavioral phenotype—dorsal body bending phenotype see upon optogenetic
470 activation of *eve*(-) ELs in Figure 9. Regardless of the exact anatomical changes, the data in
471 Figure 9 show that output synapses of *eve*(-) ELs are functional, but are functionally re-mapped
472 to new output circuits.
473
474 **Conclusion**
475 We have provided an updated understanding of the role of *eve* in neurons. Our data provide
476 understanding of the role of neuronal *eve* at the levels of circuit physiology and animal behavior.
477 Further they provide insight into the genetic logic of somatosensory circuit assembly,
478 demonstrating that multiple terminal neuronal features can be coordinately regulated by the
479 activity of a single post-mitotic transcription factor. Finally, our data raises new questions about
480 the role of *eve* in other neuron types and enable future experimental inquiry into somatosensory
481 circuit assembly in Drosophila.
482
483
484

485 **References**

486 Broihier HT, Skeath JB. Drosophila homeodomain protein dHb9 directs neuronal fate via
487 crossrepressive and cell-nonautonomous mechanisms. *Neuron*. 2002;35(1):39-50.
488 doi:10.1016/s0896-6273(02)00743-2

489 Chen, Y., Akin, O., Nern, A., Tsui, C.Y., Pecot, M.Y., Zipursky, S.L. (2014). Cell-type-
490 Specific Labeling of Synapses In Vivo through Synaptic Tagging with
491 Recombination. Neuron 81(2): 280--293.

492 Clark, M.Q., Zarin, A.A., Carreira-Rosario, A. *et al.* Neural circuits driving larval
493 locomotion in *Drosophila*. *Neural Dev* **13,** 6 (2018). https://doi.org/10.1186/s13064-018-
494 0103-z.

495 Couton L, Mauss AS, Yunusov T, Diegelmann S, Evers JF, Landgraf M. Development of
496 connectivity in a motoneuronal network in Drosophila larvae. *Curr Biol*. 2015;25(5):568-
497 576. doi:10.1016/j.cub.2014.12.056.

498 D'Elia KP, Dasen JS. Development, functional organization, and evolution of vertebrate
499 axial motor circuits. Neural Dev. 2018 Jun 1;13(1):10. doi: 10.1186/s13064-018-0108-7.
500 PMID: 29855378; PMCID: PMC5984435.

501 Doe CQ, Smouse D, Goodman CS. Control of neuronal fate by the Drosophila
502 segmentation gene even-skipped. Nature. 1988 May 26;333(6171):376-8. doi:
503 10.1038/333376a0. PMID: 3374572.

504 Emerson MM, Long JB, Van Vactor D. Drosophila semaphorin2b is required for the axon
505 guidance of a subset of embryonic neurons. Dev Dyn. 2013 Jul;242(7):861-73. doi:
506 10.1002/dvdy.23979. Epub 2013 May 30. PMID: 23606306; PMCID: PMC3739952.

507 Esmaeili B, Ross JM, Neades C, Miller DM 3rd, Ahringer J. The C. elegans even-skipped

508 homologue, vab-7, specifies DB motoneurone identity and axon trajectory. Development.
509 2002 Feb;129(4):853-62. PMID: 11861469.
510 Evans TA, Bashaw GJ. Axon guidance at the midline: of mice and flies. *Curr Opin*
511 *Neurobiol*. 2010;20(1):79-85. doi:10.1016/j.conb.2009.12.006.
512 Frasch M, Hoey T, Rushlow C, Doyle H, Levine M. Characterization and localization of
513 the even-skipped protein of Drosophila. EMBO J. 1987 Mar;6(3):749-59. PMID: 2884106;
514 PMCID: PMC553460.
515 Ferrier DE, Minguillón C, Cebrián C, Garcia-Fernàndez J. Amphioxus Evx genes:
516 implications for the evolution of the Midbrain-Hindbrain Boundary and the chordate
517 tailbud. Dev Biol. 2001 Sep 15;237(2):270-81. doi: 10.1006/dbio.2001.0375. PMID:
518 11543613.
519 Fujioka M, Emi-Sarker Y, Yusibova GL, Goto T, Jaynes JB. Analysis of an even-skipped
520 rescue transgene reveals both composite and discrete neuronal and early blastoderm
521 enhancers, and multi-stripe positioning by gap gene repressor gradients. Development.
522 1999 Jun;126(11):2527-38. PMID: 10226011; PMCID: PMC2778309.
523 Fujioka M, Lear BC, Landgraf M, Yusibova GL, Zhou J, Riley KM, Patel NH, Jaynes JB.
524 Even-skipped, acting as a repressor, regulates axonal projections in Drosophila.
525 Development. 2003 Nov;130(22):5385-400. doi: 10.1242/dev.00770. Epub 2003 Sep 16.
526 PMID: 13129849; PMCID: PMC2709291.
527 Hattori, Y., Sugimura, K. and Uemura, T. (2007), Selective expression of Knot/Collier, a
528 transcriptional regulator of the EBF/Olf-1 family, endows the *Drosophila* sensory system
529 with neuronal class-specific elaborated dendritic patterns. Genes to Cells, 12: 1011-
530 1022. https://doi.org/10.1111/j.1365-2443.2007.01107.x.

Heckscher ES, Long F, Layden MJ, Chuang CH, Manning L, Richart J, Pearson JC, Crews ST, Peng H, Myers E, Doe CQ. Atlas-builder software and the eNeuro atlas: resources for developmental biology and neuroscience. Development. 2014 Jun;141(12):2524-32. doi: 10.1242/dev.108720. PMID: 24917506; PMCID: PMC4050700.

Heckscher ES, Zarin AA, Faumont S, Clark MQ, Manning L, Fushiki A, Schneider-Mizell CM, Fetter RD, Truman JW, Zwart MF, Landgraf M, Cardona A, Lockery SR, Doe CQ. Even-Skipped(+) Interneurons Are Core Components of a Sensorimotor Circuit that Maintains Left-Right Symmetric Muscle Contraction Amplitude. Neuron. 2015 Oct 21;88(2):314-29. doi: 10.1016/j.neuron.2015.09.009. Epub 2015 Oct 1. PMID: 26439528; PMCID: PMC4619170.

Hwang, R.Y., Zhong, L., Xu, Y., Johnson, T., Zhang, F., Deisseroth, K., Tracey, W.D. (2007). Nociceptive neurons protect Drosophila larvae from parasitoid wasps. Curr. Biol. 17(24): 2105--2116.

Jinushi-Nakao, S., Arvind, R., Amikura, R., Kinameri, E., Liu, A.W., Moore, A.W. (2007). Knot/Collier and cut control different aspects of dendrite cytoskeleton and synergize to define final arbor shape. Neuron 56(6): 963--978.

Juárez-Morales JL, Schulte CJ, Pezoa SA, Vallejo GK, Hilinski WC, England SJ, de Jager S, Lewis KE. Evx1 and Evx2 specify excitatory neurotransmitter fates and suppress inhibitory fates through a Pax2-independent mechanism. Neural Dev. 2016 Feb 19;11:5. doi: 10.1186/s13064-016-0059-9. PMID: 26896392; PMCID: PMC4759709.

Kohsaka H, Guertin PA, Nose A. Neural Circuits Underlying Fly Larval Locomotion. *Curr Pharm Des*. 2017;23(12):1722-1733. doi:10.2174/1381612822666161208120835.

Kurmangaliyev YZ, Yoo J, LoCascio SA, Zipursky SL. Modular transcriptional programs

554 separately define axon and dendrite connectivity. *Elife*. 2019;8:e50822. Published 2019
555 Nov 5. doi:10.7554/eLife.50822.
556 Lai HC, Seal RP, Johnson JE. Making sense out of spinal cord somatosensory
557 development. Development. 2016 Oct 1;143(19):3434-3448. doi: 10.1242/dev.139592.
558 PMID: 27702783; PMCID: PMC5087618.
559 Landgraf M, Roy S, Prokop A, VijayRaghavan K, Bate M. even-skipped determines the
560 dorsal growth of motor axons in Drosophila. Neuron. 1999 Jan;22(1):43-52. doi:
561 10.1016/s0896-6273(00)80677-7. PMID: 10027288.
562 Landgraf M, Sánchez-Soriano N, Technau GM, Urban J, Prokop A. Charting the
563 Drosophila neuropile: a strategy for the standardised characterisation of genetically
564 amenable neurites. Dev Biol. 2003 Aug 1;260(1):207-25. doi: 10.1016/s0012-
565 1606(03)00215-x. PMID: 12885565.
566 Lee EJ, Kim N, Park JW, Kang KH, Kim WI, Sim NS, Jeong CS, Blackshaw S, Vidal M,
567 Huh SO, Kim D, Lee JH, Kim JW. Global Analysis of Intercellular Homeodomain Protein
568 Transfer. Cell Rep. 2019 Jul 16;28(3):712-722.e3. doi: 10.1016/j.celrep.2019.06.056.
569 PMID: 31315049.
570 Meng JL, Heckscher ES. Development of motor circuits: From neuronal stem cells and
571 neuronal diversity to motor circuit assembly. Curr Top Dev Biol. 2021;142:409-442. doi:
572 10.1016/bs.ctdb.2020.11.010. Epub 2020 Dec 19. PMID: 33706923.
573 Meng JL, Marshall ZD, Lobb-Rabe M, Heckscher ES. How prolonged expression of
574 Hunchback, a temporal transcription factor, re-wires locomotor circuits. Elife. 2019 Sep
575 10;8:e46089. doi: 10.7554/eLife.46089. PMID: 31502540; PMCID: PMC6754208.
576 Meng, J. L., Wang, Y., Carrillo, R. A., & Heckscher, E. S. (2020). Temporal transcription

577 factors determine circuit membership by permanently altering motor neuron-to-muscle
578 synaptic partnerships. (), 2020.03.25.007252. Accessed April 30, 2021.
579 https://doi.org/10.1101/2020.03.25.007252.
580 Moran-Rivard L, Kagawa T, Saueressig H, Gross MK, Burrill J, Goulding M. Evx1 is a
581 postmitotic determinant of v0 interneuron identity in the spinal cord. Neuron. 2001
582 Feb;29(2):385-99. doi: 10.1016/s0896-6273(01)00213-6. PMID: 11239430.
583 Nern A, Pfeiffer BD, Rubin GM. Optimized tools for multicolor stochastic labeling reveal
584 diverse stereotyped cell arrangements in the fly visual system. Proc Natl Acad Sci U S A.
585 2015 Jun 2;112(22):E2967-76. doi: 10.1073/pnas.1506763112. Epub 2015 May 11. PMID:
586 25964354; PMCID: PMC4460454.
587 Ohyama T, Schneider-Mizell CM, Fetter RD, Aleman JV, Franconville R, Rivera-Alba M,
588 Mensh BD, Branson KM, Simpson JH, Truman JW, Cardona A, Zlatic M. A multilevel
589 multimodal circuit enhances action selection in Drosophila. Nature. 2015 Apr
590 30;520(7549):633-9. doi: 10.1038/nature14297. Epub 2015 Apr 20. PMID: 25896325.
591 Parrish JZ, Kim MD, Jan LY, Jan YN. Genome-wide analyses identify transcription factors
592 required for proper morphogenesis of Drosophila sensory neuron dendrites. *Genes Dev*.
593 2006;20(7):820-835. doi:10.1101/gad.1391006.
594 Pym EC, Southall TD, Mee CJ, Brand AH, Baines RA. The homeobox transcription factor
595 Even-skipped regulates acquisition of electrical properties in Drosophila neurons. Neural
596 Dev. 2006 Nov 16;1:3. doi: 10.1186/1749-8104-1-3. PMID: 17147779; PMCID:
597 PMC1679800.
598 Rexed, B. (1952), The cytoarchitectonic organization of the spinal cord in the cat. J. Comp.
599 Neurol., 96: 415-495. https://doi.org/10.1002/cne.900960303.

600 Risse B, Berh D, Otto N, Klämbt C, Jiang X. FIMTrack: An open source tracking and
601 locomotion analysis software for small animals. PLoS Comput Biol. 2017 May
602 11;13(5):e1005530. doi: 10.1371/journal.pcbi.1005530. PMID: 28493862; PMCID:
603 PMC5444858.
604 Santiago C, Bashaw GJ. Transcription factors and effectors that regulate neuronal
605 morphology. Development. 2014 Dec;141(24):4667-80. doi: 10.1242/dev.110817. PMID:
606 25468936; PMCID: PMC4299270.
607 Sholl DA. Dendritic organization in the neurons of the visual and motor cortices of the
608 cat. *J Anat.* 1953;87:387–406.
609 Stratmann, J., Ekman, H., Thor, S. (2019). A branching gene regulatory network dictating
610 different aspects of a neuronal cell identity.
611 Valdes-Aleman J, Fetter RD, Sales EC, Heckman EL, Venkatasubramanian L, Doe CQ,
612 Landgraf M, Cardona A, Zlatic M. Comparative Connectomics Reveals How Partner
613 Identity, Location, and Activity Specify Synaptic Connectivity in Drosophila. Neuron.
614 2021 Jan 6;109(1):105-122.e7. doi: 10.1016/j.neuron.2020.10.004. Epub 2020 Oct 28.
615 PMID: 33120017; PMCID: PMC7837116.
616 Wagh, D.A., Rasse, T.M., Asan, E., Hofbauer, A., Schwenkert, I., Duerrbeck, H., Buchner,
617 S., Dabauvalle, M.C., Schmidt, M., Qin, G., Wichmann, C., Kittel, R., Sigrist, S.J.,
618 Buchner, E. (2006). Bruchpilot, a protein with homology to ELKS/CAST, is required for
619 structural integrity and function of synaptic active zones in Drosophila. Neuron 49(6): 833-
620 -844.
621 Wreden CC, Meng JL, Feng W, Chi W, Marshall ZD, Heckscher ES. Temporal Cohorts of
622 Lineage-Related Neurons Perform Analogous Functions in Distinct Sensorimotor Circuits.

623 Curr Biol. 2017 May 22;27(10):1521-1528.e4. doi: 10.1016/j.cub.2017.04.024. Epub 2017
624 May 11. PMID: 28502656.
625 Zarin AA, Asadzadeh J, Hokamp K, McCartney D, Yang L, Bashaw GJ, Labrador JP. A
626 transcription factor network coordinates attraction, repulsion, and adhesion combinatorially
627 to control motor axon pathway selection. Neuron. 2014 Mar 19;81(6):1297-1311. doi:
628 10.1016/j.neuron.2014.01.038. Epub 2014 Feb 20. PMID: 24560702; PMCID:
629 PMC4128230.
630 Zeilig G, Enosh S, Rubin-Asher D, Lehr B, Defrin R. The nature and course of sensory
631 changes following spinal cord injury: predictive properties and implications on the
632 mechanism of central pain. *Brain*. 2012;135(Pt 2):418-430. doi:10.1093/brain/awr270
633 Zlatic M, Landgraf M, Bate M. Genetic specification of axonal arbors: atonal regulates
634 robo3 to position terminal branches in the Drosophila nervous system. *Neuron*.
635 2003;37(1):41-51. doi:10.1016/s0896-6273(02)01131-5.
636 Zlatic M, Li F, Strigini M, Grueber W, Bate M. Positional cues in the Drosophila nerve
637 cord: semaphorins pattern the dorso-ventral axis. PLoS Biol. 2009 Jun 16;7(6):e1000135.
638 doi: 10.1371/journal.pbio.1000135. Epub 2009 Jun 23. PMID: 19547742; PMCID:
639 PMC2690435.
640
641
642

643 **Figures**

644 **Figure 1. In EL eve mutants, EL interneurons lack Eve expression**

645 **A-B. Images of Eve expression in the nerve cord of Drosophila embryos.** A. In control, each
646 segment has *eve*(+) motor neurons (MNs, red) and *eve*(+) EL interneurons (INs, green). B. In EL
647 eve mutants, Eve is selectively lost from EL, but neurons themselves remain (*Fujioka et al.,*
648 *2003*). Images show Eve expression in three segments of the Drosophila nerve cord of stage 16
649 embryos. Anterior is up with scale bar of 15 microns. Position of EL interneurons in one
650 hemisegment is circled. Midline is marked by an arrowhead.

651 **C-D. Schematics of genomic constructs that rescue *eve* expression**. C. The top line shows a
652 wild type "WT eve" genomic DNA fragment (EGN92, *Fujioka et al., 2003*), which contains all
653 known *eve* coding and regulatory sequences. The bottom line represents the "ΔEL" rescue
654 construct, which is identical to WT *eve* construct except it lacks the EL enhancer (EGN92 ΔEL,
655 *Fujioka et al., 2003*). D. Two different *eve* null alleles (*Df(2R)eve* and *eve(3)*) are rescued with
656 the ΔEL construct, referred to EL eve mutant (1) and EL eve mutant (2), respectively.
657 **Genotypes:** Control is Δ*EL, Df(2R)eve/+* and EL eve mutant is Δ*EL, eve(3)/* Δ*EL, Df(2R)ev*e.
658

659 **Figure 2. In embryos, *eve* is required for proper medial-lateral and anterior-posterior**
660 **neurite positioning of EL interneurons**

661 **A-C. Images and quantification of stage 15 embryos with EL interneurons extending axons**
662 **across the midline**. A-B. In control and EL eve mutants, ELs extend across the midline. Two
663 abdominal segments are shown with midline noted as an arrowhead. Anterior is up and scale bars
664 are 10 microns. Below each image is an illustration of the phenotype. C. For this quantification,

n = number of hemisegments with EL processes crossing the midline over the total number of hemisegments scored.

D-F. Images and quantification of stage 16 embryos with defects in medial-lateral positioning of EL neurites in EL eve mutants. D. In control, ELs project toward the anterior mainly along the intermediate fascicle. E. In EL eve mutants, ELs project in additional fascicles (arrows).(L = lateral fascicle, I = intermediate, M = medial). F, For this quantification, n = number of hemisegments scored.

G-I. Images and quantification of stage 17 embryos, with defects in anterior-posterior positioning of EL neurites in EL eve mutants. G. In control, ELs extend neurites to the next anterior segment. H. In EL eve mutants, neurites do not extend to the next segment (arrow). I. For this quantification, n = number of hemisegments with processes reaching the next segment over the total number of hemisegments scored. Chi-square **** $P < 0.0001$.

Genotypes: Control 1 is *EL-GAL4/UAS-myr-GFP.* Control 2 is *UAS-FLP, act5C-FRT.stop-GAL4;;EL-GAL4/UAS-myr-GFP*. EL eve mutant (1) is *UAS-FLP, act5C-FRT.stop-GAL4; ΔEL, Df(2R)eve/ΔEL, Df(2R)eve; EL-GAL4/UAS-myr-GFP*.

Figure 3. In larvae, *eve*(-) ELs have excessive branching off the main neurite and diminished axon extension

A. Quantification of labeled neurons. In all genotypes, the most numerous type of singly-labeled neurons are local, late-born ELs. n = total number of singly-labeled neurons for each genotype.

B-C. Images of singly-labeled ELs. Drosophila neurons are pseudo-unipoloar. B. In control, dendrites are located ipsilateral to the soma. On the contralateral side, axons turn to the anterior

and form branches where output synapses are found (*Heckscher et al., 2015*). C. In EL eve mutants, there is excessive branching off the main neurite (arrowheads), and the axon is less extended (arrow). Anterior is up with a scale bar of 5 microns. Dashed line indicates midline. **D-G. Quantifications of neuron morphology.** For each plot, the X-axis is the radius of a concentric circle centered on the EL soma. The Y-axis is number of times a singly-labeled EL intersects a circle. Median (dark line) and range (lighter bars) are shown. F. Control is black; red and orange lines are EL eve mutants (1) and (2), respectively. Wilcoxon test, *** P <0.0001. **Genotypes:** Control is *11F02-GAL4/UAS-MCFO*. EL eve mutant (1) is Δ*EL, Df(2R)eve/*Δ*EL, Df(2R)eve; 11F02-GAL4/UAS-MCFO.* EL eve mutant (2) is Δ*EL, Df(2R)eve/*Δ*EL, eve(3); 11F02-GAL4/UAS-MCFO*.

Figure 4. *eve*(-) ELs have mispositioned dorsal-ventral dendrites

A-B. Images of singly-labeled ELs in side view. A. In control, ELs have ipsilateral dendrites that project dorsally. B. In EL eve mutants, many branches project ventrally. These are the same neurons as in Figure 3B-C, except here dorsal is up.

C-D. Quantification of dendrite orientation. The number of branches pointing dorsally or ventrally is plotted with each dot representing a single neuron. Bars show average, and whiskers show standard deviation. ANOVA with Dunnett's multiple comparison * is P <0.05 and **** is P <0.0001.

Figure 5. ***eve*(-) ELs do not derepress molecular markers**

A-D. Images of marker gene expression in ELs. A, C. In control, ELs lack expression of ventral motor neuron maker, HB9 (A') and an interneuron marker En (A''). ELs express both

711 Eagle (C') and Collier (C"). B, D. In EL eve mutants, there is no change in marker gene
712 expression. Representative segments of stage 16 embryos. Anterior is up with a scale bar of 5
713 microns. Arrowhead shows midline. Area containing EL neurons is circled. n = number of
714 hemisegments scored. Each row shows separate image channels of the same co-stained stained
715 embryo.
716 **Genotypes:** Control is *wild-type* and EL eve mutant(1) is *ΔEL, Df(2R)eve/ΔEL, eve(3).*
717
718 **Figure 6. In EL eve mutants, there are no changes in sensory neurons axonal trajectories**
719 **A-B. Illustration of sensory inputs onto ELs.** A. Late-born ELs get direct input from
720 proprioceptors and indirect input via the Jaam CNS interneurons. B. Early-born ELs get direct
721 input from mechanoreceptors (chordotonals) and indirect input via the Basin CNS interneurons.
722 **C-F. Illustrations of sensory neuron-to-interneuron wiring in different genetic conditions.**
723 C. In wild type, sensory neuron axons (green) and interneuron dendrites (blue) are in close
724 enough proximity they can form synaptic contacts. D. When sensory neuron axons are
725 genetically mispositioned, interneurons grow in response, and the two cell types continue to form
726 synaptic contacts. E-F. When EL interneuron dendrites are mispositioned due to lack of Eve,
727 sensory neurons might or might not change position in response.
728 **G-H. Images of vibration and proprioceptive sensory neurons arbors**. G-H. Axonal positions
729 are similar in control and EL eve mutants for both vibration sensitive and proprioceptive sensory
730 neurons. Single hemisegments of an L1 larval CNS are shown with dorsal up. Eve-expressing
731 motor neurons are shown as solid circles with a diameter of five microns. Positions of Fas2(+)
732 fascicles are shown as dashed circles. To the left of each image is a schematic of the axon
733 position relative to landmarks. n = the number of hemisegments scored.

Genotypes: Control in G is *iav-GAL4/UAS-myr-GFP.* EL eve mutant in G is Δ*EL, Df(2R)eve/*Δ*EL, Df(2R)eve; iav-GAL4/UAS-myr-GFP.* Control in H is *0165-GAL4/UAS-myr-GFP.* EL eve mutant in H is Δ*EL, Df(2R)eve/*Δ*EL, Df(2R)eve; 0165-GAL4/UAS-myr-GFP.*

Figure 7. EL interneurons require *eve* to encode somatosensory stimuli

A. Illustration of the semi-restrained preparation and stimulus protocol. Fluorescence in the CNS (gray lobed structure with two white lines [neuropile]) is recorded before, during, and after a sound is played from a speaker.

B-C. Quantifications of EL calcium signals. B. In control, EL have small amplitude, dynamic calcium signals before sound onset, which corresponds to periods of self-movement. There are large amplitude changes in EL calcium signal upon sound/vibration stimuli. C. In EL eve mutants, ELs do not respond to stimuli. Averages (dark line) and SEM (light line) are shown. Scale for both is shown as an inset. n = number of larvae recorded.

D-E. Images from representative recordings of calcium signals in ELs. D-E. Fluorescence images are shown in pseudo-color with white/red as high fluorescence intensity and blue as low. Anterior is up with a scale bar of 100 microns. Dashed lines show the outline of the nerve cord. In D, asterisk denotes region of nerve cord neuropile (central region) with increased fluorescence. In, E ">" points to mouth hooks.

Genotypes: Control is *UAS-FLP, act5C-FRT.stop-GAL4;* Δ*EL, Df(2R)eve/+; EL-GAL4/UAS-GCaMP6m.* EL eve mutant is *UAS-FLP, act5C-FRT.stop-GAL4;* Δ*EL, Df(2R)eve/*Δ*EL, Df(2R)eve; EL-GAL4/UAS-GCaMP6m.*

Figure 8. In *eve*(-) ELs, output synapses are anatomically repositioned.

A-B. Images of tagged pre-synaptic active zones. Eve labels ELs ("ELs" in A) but not in EL eve mutants (* in B). A'. In control, labeled active zones (BRP) are clustered around the central intermediate Fas2(+) fascicles ("CI"). B'. In EL eve mutants, BRP signal is diffuse throughout the entire neuropile. A-A'' are the same CNS and B-B" are the same CNS. A" and B" are a magnifications of the neuropile from one hemisegment in A' or B', respectively. Images are overlaid with lines showing medial (M), intermediate (I), and lateral (L) zones. Images show the CNS in cross section with dorsal up. Arrow denotes midline. Neuropile is outlined by a dashed circle. Scale bar is 10 microns.

C-D. Quantifications of BRP signal distribution. n= number of hemisegments with BRP signal above background within a given region /total number of hemisegments scored. Zones scored were medial (M), intermediate (I), and lateral (L) as shown in A'' and B''.

Genotype: Control is *UAS-FLP, act5C-FRT.stop-GAL4; ΔEL, Df(2R)eve/+; EL-GAL4/UAS-FLP, BRP-frt-stop-frt-V5-2A-LexA.* EL eve mutant is *UAS-FLP, act5C-FRT.stop-GAL4; ΔEL, Df(2R)eve/ΔEL, Df(2R)eve; EL-GAL4/UAS-FLP, BRP-frt-stop-frt-V5-2A-LexA. ΔEL*

ΔEL

Figure 9. In EL eve mutants, there are defects in spontaneously-occurring crawling behavior.

A-C. Images and quantification of larva crawling. A-B. Images of control and EL eve mutants during forward crawling. Images are frames (0.66 second intervals) from representative behavioral recordings. Anterior is up and scale bar is 150 microns. C. Quantification of crawling speed is calculated as centroid movement over time. Each dot represents the average data for one

779 larva. Bars represent average of all data points, and whiskers show SEM. One-way ANOVA
780 with Dunnett's multiple comparison **P <0.01; **** P <0.0001.
781 **D-F. Images of left-right asymmetrical body posture.** D. In control, larvae crawl left-right
782 symmetrically. E. When ELs are genetically ablated during embryogenesis, larvae crawl with
783 left-right asymmetrical body posture. F. In EL eve mutants, when Eve is removed from ELs, but
784 the EL neurons remain, larvae crawl with a significantly severe left-right asymmetrical body
785 posture. Images are single representative frames from behavioral recordings showing body shape
786 with anterior up, and scale bar of 40 microns. F is overlaid to show how angles are calculated.
787 **G-H. Quantification of left-right body asymmetry.** Asymmetry is measured as tail-to-centroid
788 and head-to-centroid angles during crawling. Each dot represents the average data for one larva.
789 Data for No ELs replotted from Heckscher et al., 2015, with permission. Bars represent average
790 of all data points, and whiskers show SEM. ANOVA with Dunnett's multiple comparison test
791 **P <0.01; **** P <0.0001.
792 **Genotypes**: Control is Δ*EL, Df(2R)eve/+*. No EL is *UAS-RPR, UAS-HID/+; ; EL-GAL4/+*. EL
793 eve mutant is Δ*EL, Df(2R)eve)/*Δ*EL, Df(2R)eve.*
794
795 **Figure 10. EL outputs are remapped in the absence of Eve.**
796 **A-B. Images of behavioral responses to optogenetic stimulation of ELs.** A. Control larvae fed
797 all trans retinal (ATR) and expressing CsChrimson in ELs roll in response to light. B. EL eve
798 mutant larvae fed ATR and expressing CsChrimson in ELs display a novel dorsal bend
799 phenotype (can be either side). Images are frames from representative behavioral recordings
800 (shown at 0.6 second intervals). Scale bar is 150 microns. In B, ">" points to dorsal.

C. Illustration of the behavioral rig. The rig uses infrared light emitting diodes (IR LEDs) to illuminate larvae, which is detected by the camera, but not the larvae. Amber LEDs stimulate optogenetic effectors.

D-E. Quantification of larval movement. Centroid speed is calculated as centroid displacement/time. Orange bar shows exposure to amber light. Gray traces (bottom) are control larvae not fed ATR, a co-factor needed for optogenetic simulation. Black traces are experimental larvae, which were fed ATR. n = number of larvae recorded. Average is shown as darker lines and SEM is shown as lighter lines. Wilcoxon test, *** P <0.0001.

F-G. Illustrations of behavioral responses. Controls roll in response to EL activation, whereas EL eve mutants perform a dorsal bend in response to EL activation.

H-I. Quantification of larval sensorimotor transformations. H-I. Control and EL eve mutant larvae roll in response to body wall pinch and hunch in response to vibration. Illustration of each behavior is shown in top left of each panel. For quantifications, n = number of larvae responding to each stimulus over the total number of larvae stimulated. Chi-squared n.s. = not significant.

Genotype: Control in A and D is *UAS-FLP, act5C-FRT.stop-GAL4; ΔEL, Df(2R)eve/+; EL-GAL4/UAS-Cs.Chrimson.mVenus.* EL eve mutant in B and E is *UAS-FLP, act5C-FRT.stop-GAL4; ΔEL, Df(2R)eve/ΔEL, Df(2R)eve; EL-GAL4/UAS-Cs.Chrimson.mVenus.* Control in H is *ΔEL, Df(2R)eve/+*. EL eve mutant in I is *ΔEL, Df(2R)eve)/ΔEL, Df(2R)eve.*

822 Table 1. Methods used to label EL interneurons
823

Genotype		Labeling method			
		Anti-Eve	*EL-GAL4*	*UAS-FLP, actin-FRT-stop-FRT-GAL4;;EL-GAL4*	*11F02-GAL4*
Wild type	Neurons labeled	EL interneurons, Motor neurons	EL interneurons	EL interneurons	Late-born ELs, other neurons
	Stages	Neuron birth to larval L3	Embryos stage 14 to larval L2	Embryo stage 15 to larval L3	Embryo stage 15 to larval
EL eve mutant/ EL eve mutant	Neurons labeled	Motor neurons	EL interneurons	EL interneurons	Late-born ELs, other neurons
	Stages	Neuron birth to larval L3	Embryo stage 14 to stage 15	Embryo stage 15 to larva	Embryo stage 15 to larva
EL eve mutant/ *eve(5)*	Neurons labeled	EL interneurons, Motor neurons	EL interneurons	N/A	N/A
	Stages	Neuron birth to larval L3	Embryo stage 14 to larval L2	N/A	N/A

824
825

826 Table 2. Antibodies, Fly Lines
827

Antibodies (Concentration)	Source (Catalog number)
Rabbit-Eve (1:500)	Ellie Heckscher, University of Chicago (1432p)
Mouse-Eve (pre-absorbed 4µg/mL)	Developmental Studies Hybridoma Bank (DSHB) (2B8)
Mouse-FasII (1:100)	DSHB (1D4)
Rat-Flag (1:300)	Novus (Cat #NBP1-06712; RRID: AB_1625981)
Mouse-HA (1:300)	BioLegend (Cat #901501; RRID: AB_2565006)
Chicken-V5 (1:300)	Bethyl (Cat #A190-118A; RRID: AB_66741)
Chicken-GFP (1:500)	Aves & Abcam (AB_2307313 ab13970)
Guinea Pig-Hb9 (1:1000)	Heather Broihier, Case Western
Mouse-Eagle (1:50)	Abcam (ab 2013237)
Mouse-AbdA/Ubx (1:400)	DSHB (FP6.87)
Mouse-AbdB (1:400)	DSHB (1A2E9)
Mouse-En (1:5)	DSHB (4D9)
Rabbit-Cas (1:500)	Chris Doe, University of Oregon
Mouse-Cut (1:50)	DSHB (2B10)
Rat-Dpn (1:50)	Chris Doe, University of Oregon
Mouse-Islet (1:10)	DSHB (40.3A4)
Guinea Pig-Kruppel (1:1000)	John Reintz, University of Chicago
Rabbit-Nab (1:1000)	Chris Doe, University of Oregon
Guinea Pig-Knot (1:1000)	Adrian Moore, RIKEN
Rat-Pdm2 (1:100)	Chris Doe, University of Oregon
Mouse-Svp (1:500)	DSHB (6F7)
Rat-Zfh2 (1:200)	Chris Doe, University of Oregon
Mouse-Antp (1:400)	DSHB (8C11)
Mouse-Repo (1:10)	DSHB (8D12)
Fly lines	
11F02-gal4	Bloomington Drosophila Stock Center (BDSC): 9828
actin-FRT.stop-Gal4	BDSC: 4779
UAS FLP, BRP-frt-stop-frt-V5-2A-LexA	BDSC: 55749
Df(2R) eve	BDSC: 1545
eve(3)	BDSC: 299
eve(5)	BDSC: 4084
UAS-Chrimson.mVenus	BDSC: 5535
UAS-FLP	BDSC: 8208
UAS(FRT.stop)myr::smGdP-HA,UAS(FRT.stop)myr::smGdP-V5, UAS(FRT.stop)myr::smGdP-FLAG; FLPG5.PEST	BDSC: 64085
UAS-GCaMP6m	BDSC: 42786
UAS-myr-GFP	BDSC: 32197
EGN92, ΔEL_B	Fujioka, et al., 2003
EL-GAL4	Fujioka, et al., 1999
UAS-RPR, UAS-HID	Heckscher, et al. 2015

828

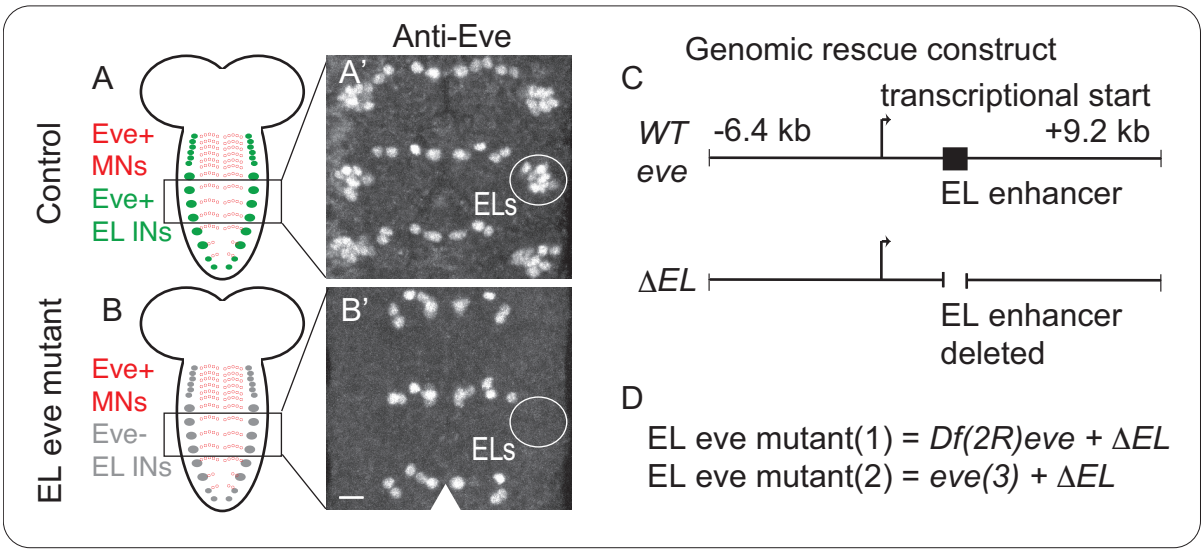

Figure 1.

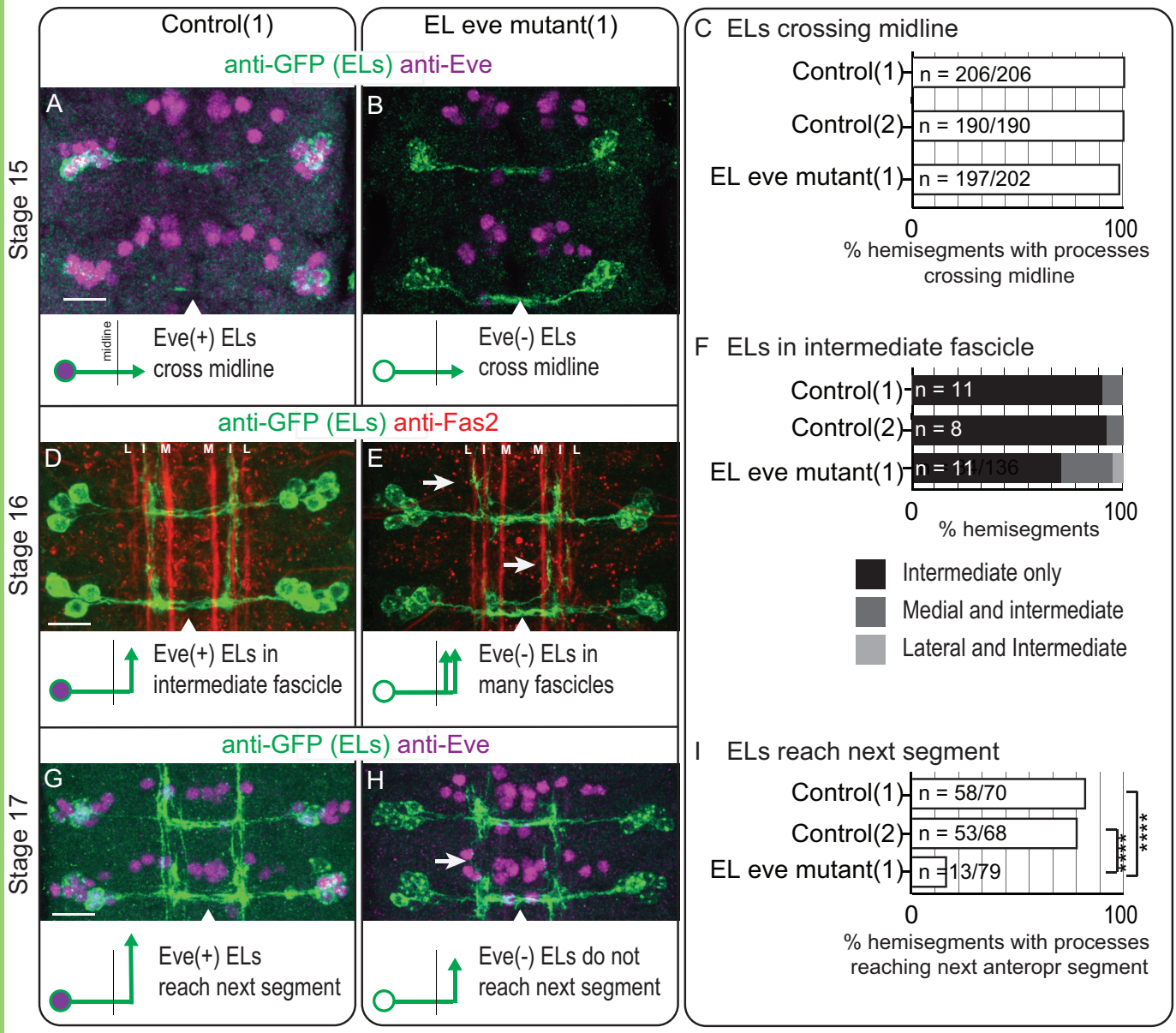

Figure 2.

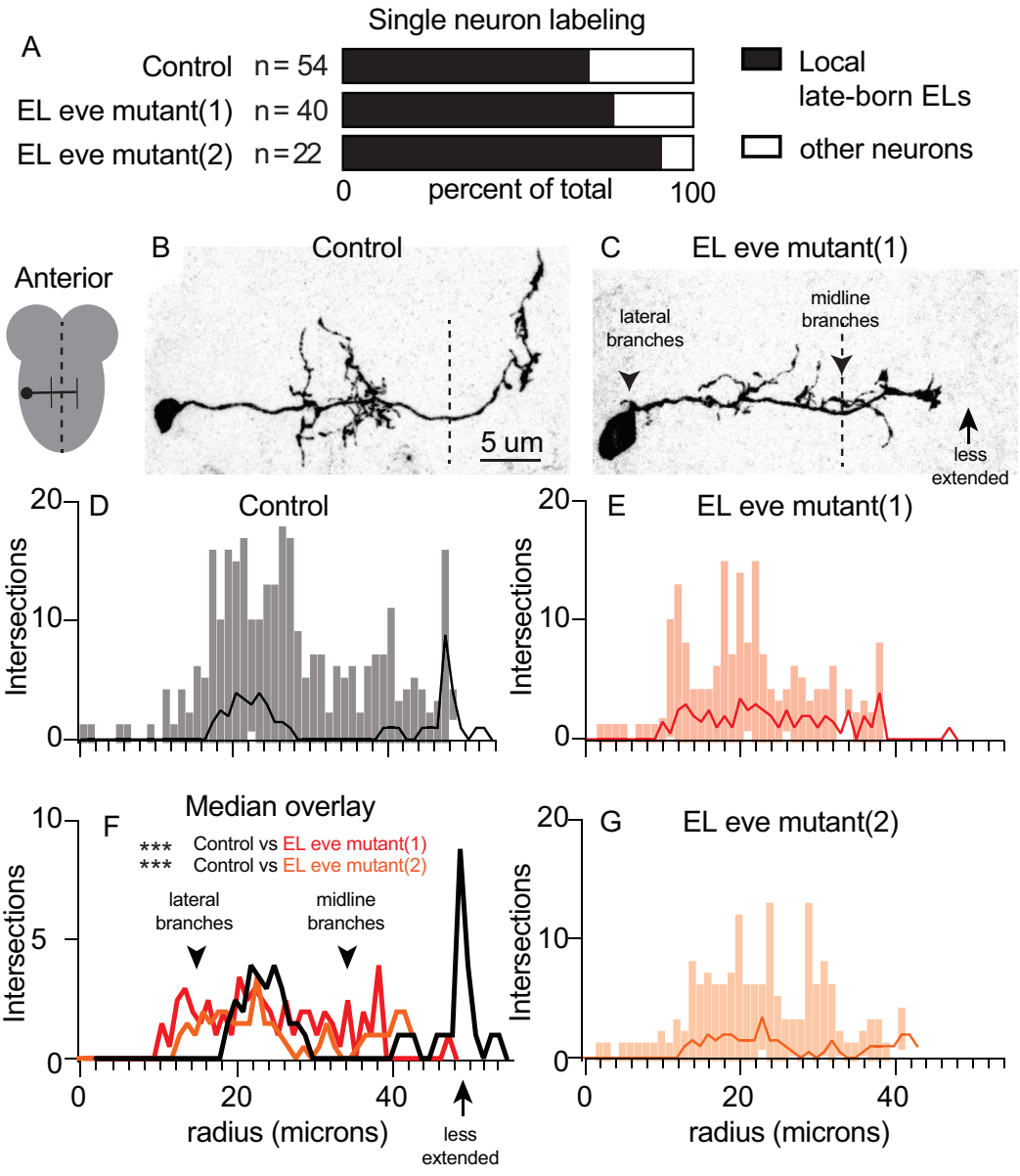

Figure 3.

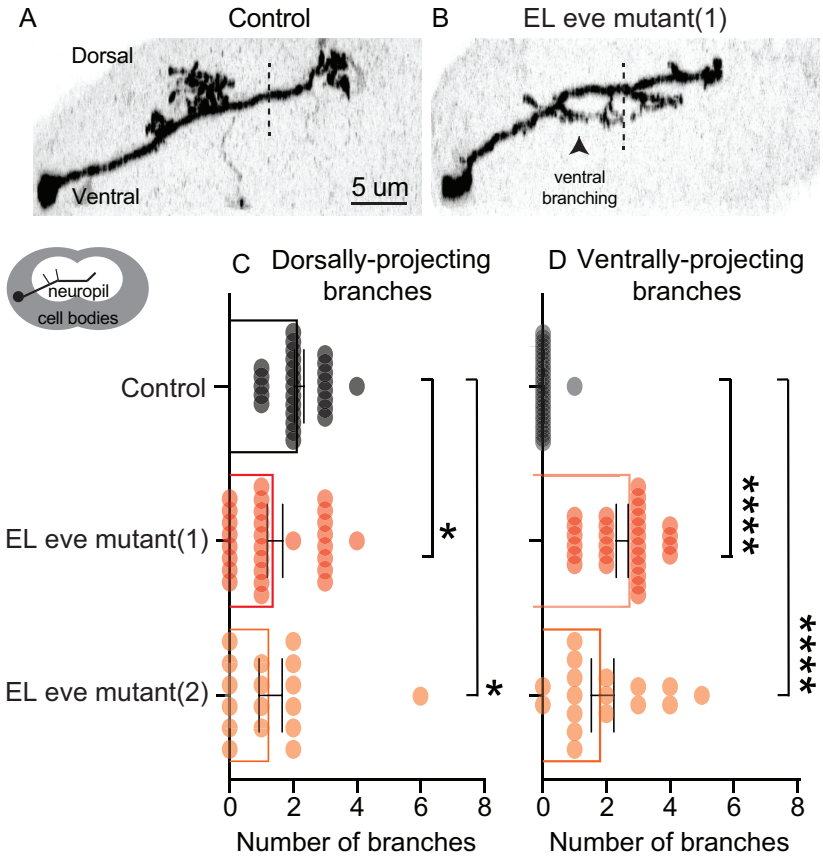

Figure 4.

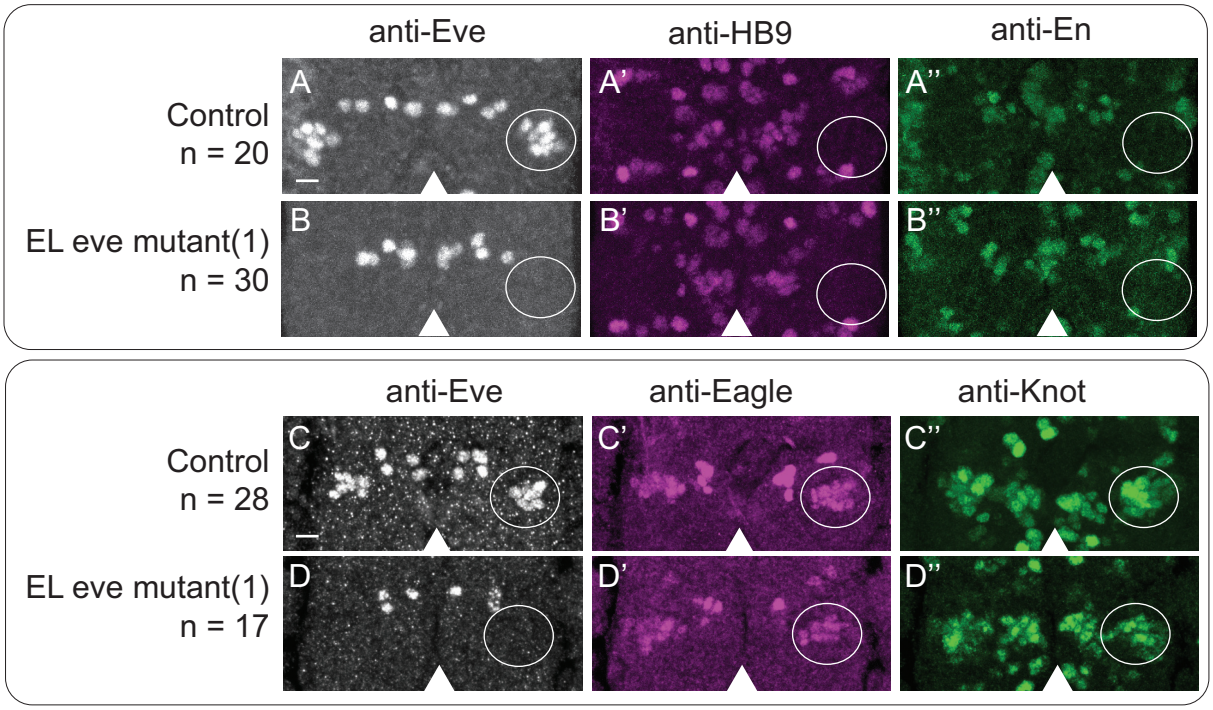

Figure 5.

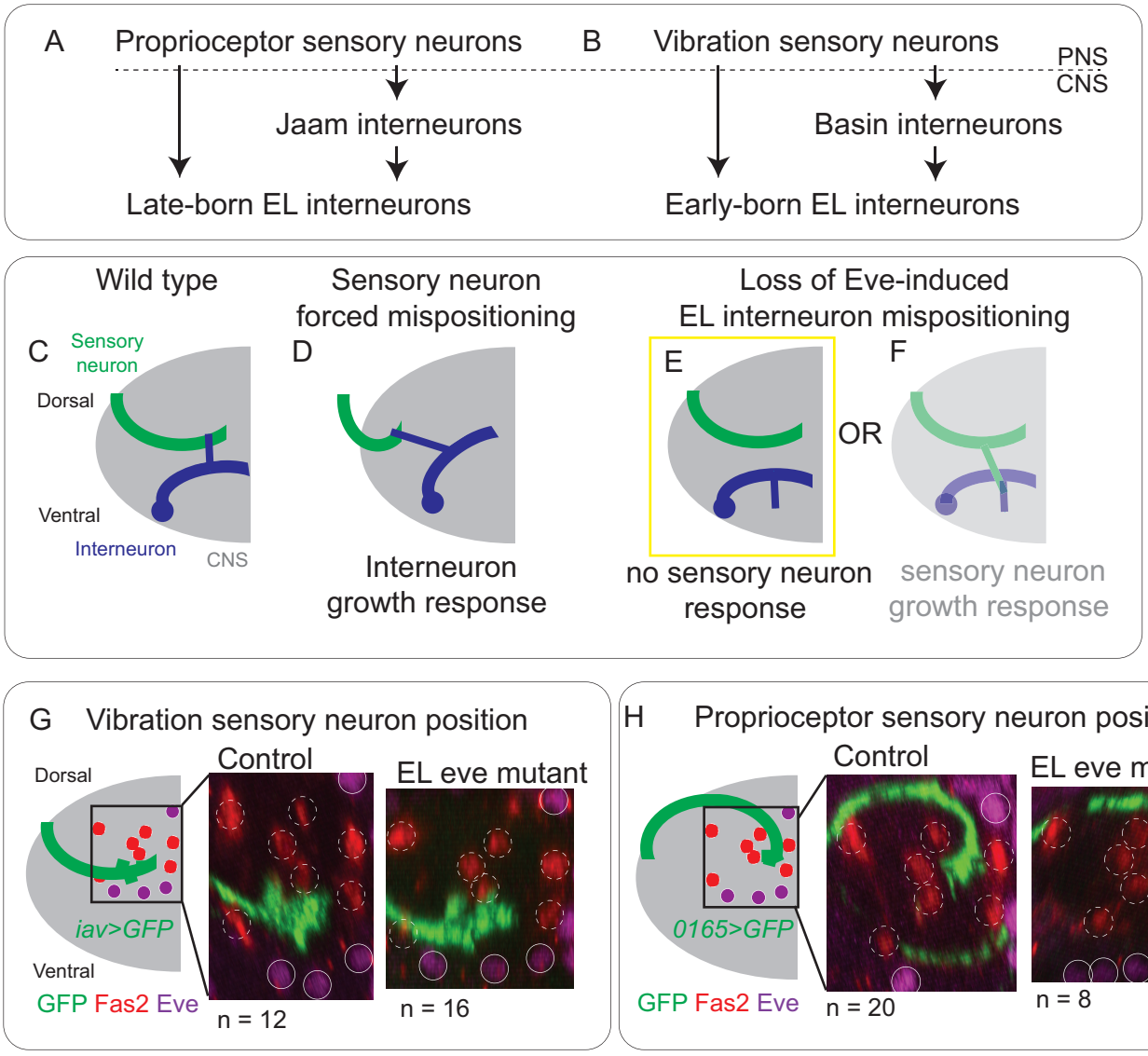

Figure 6.

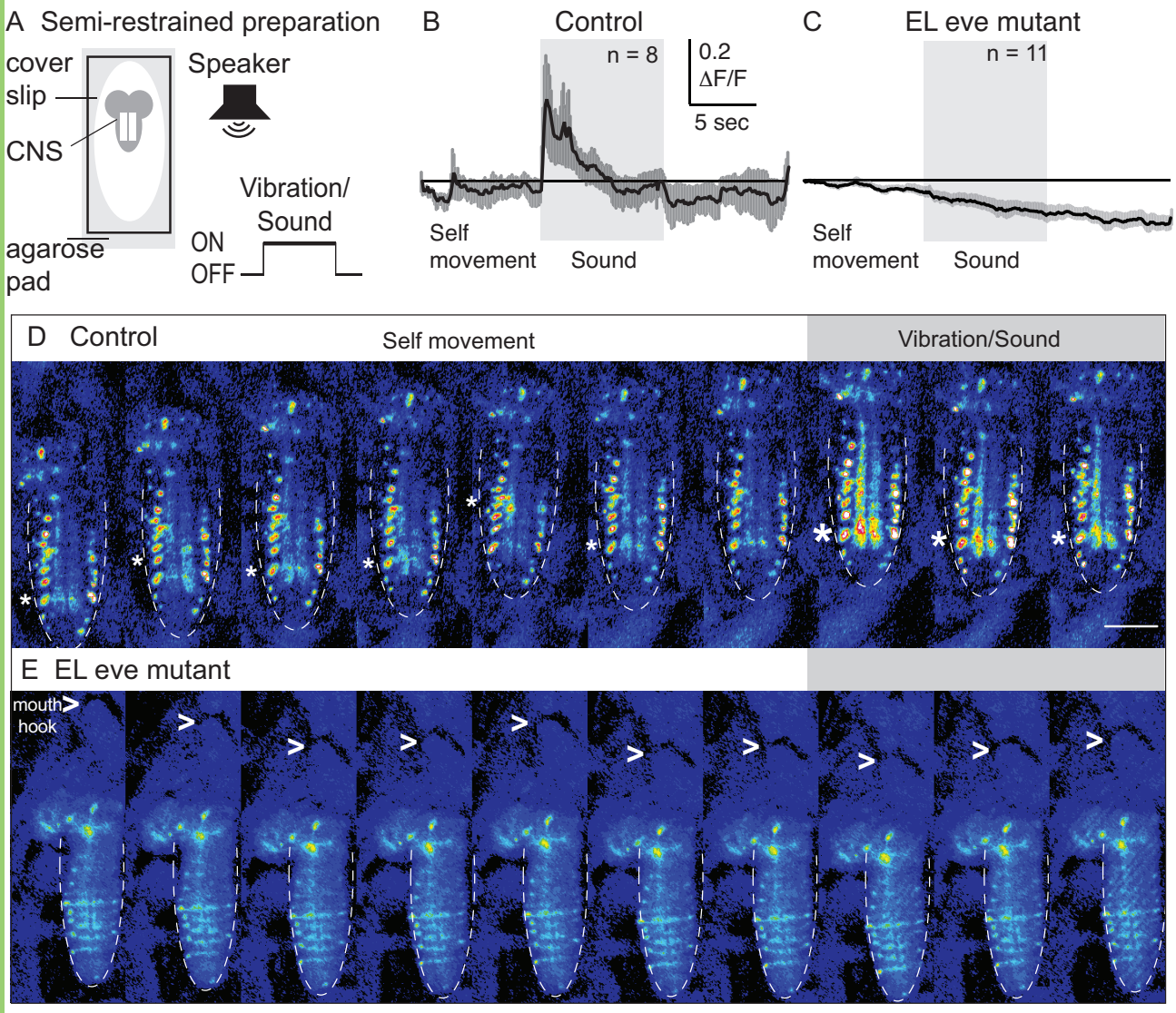

Figure 7.

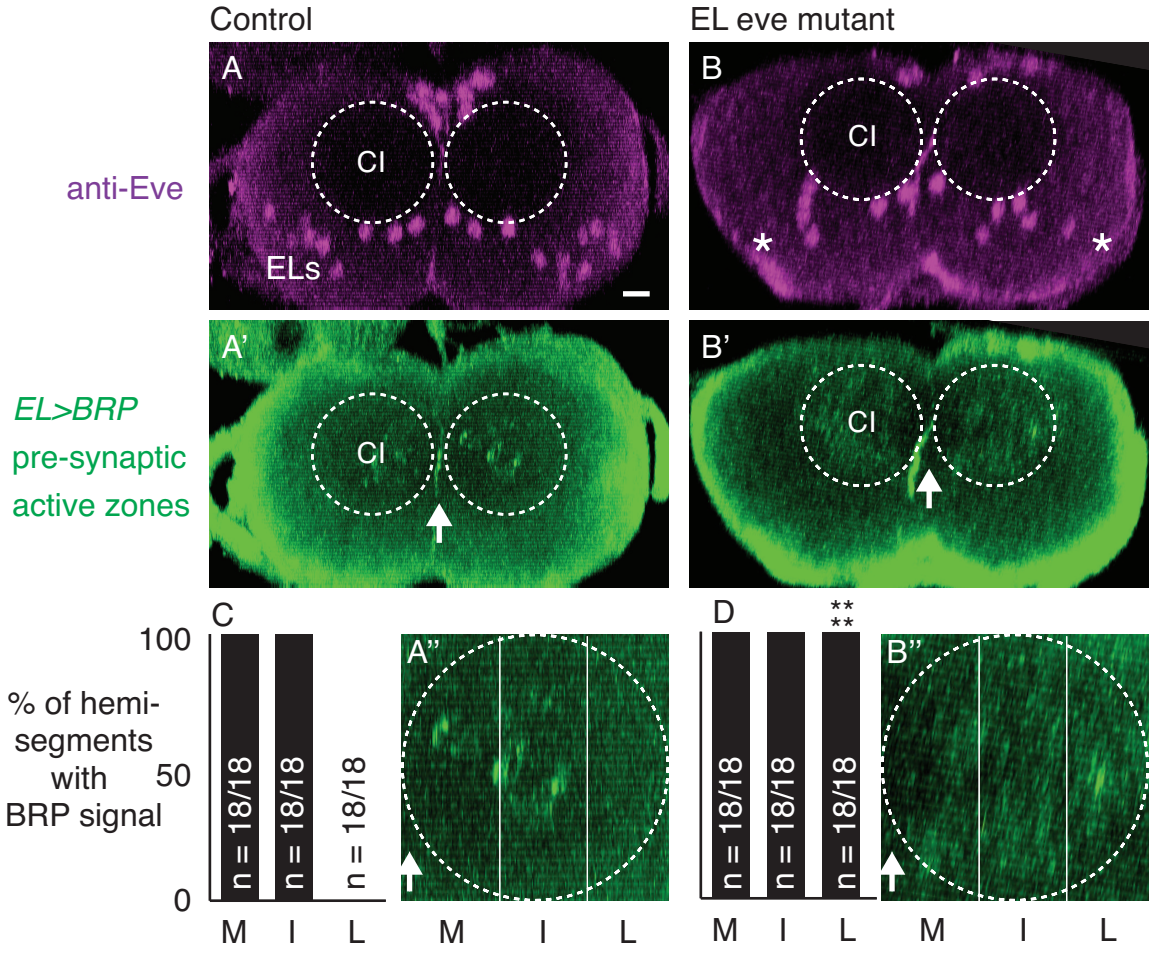

Figure 8

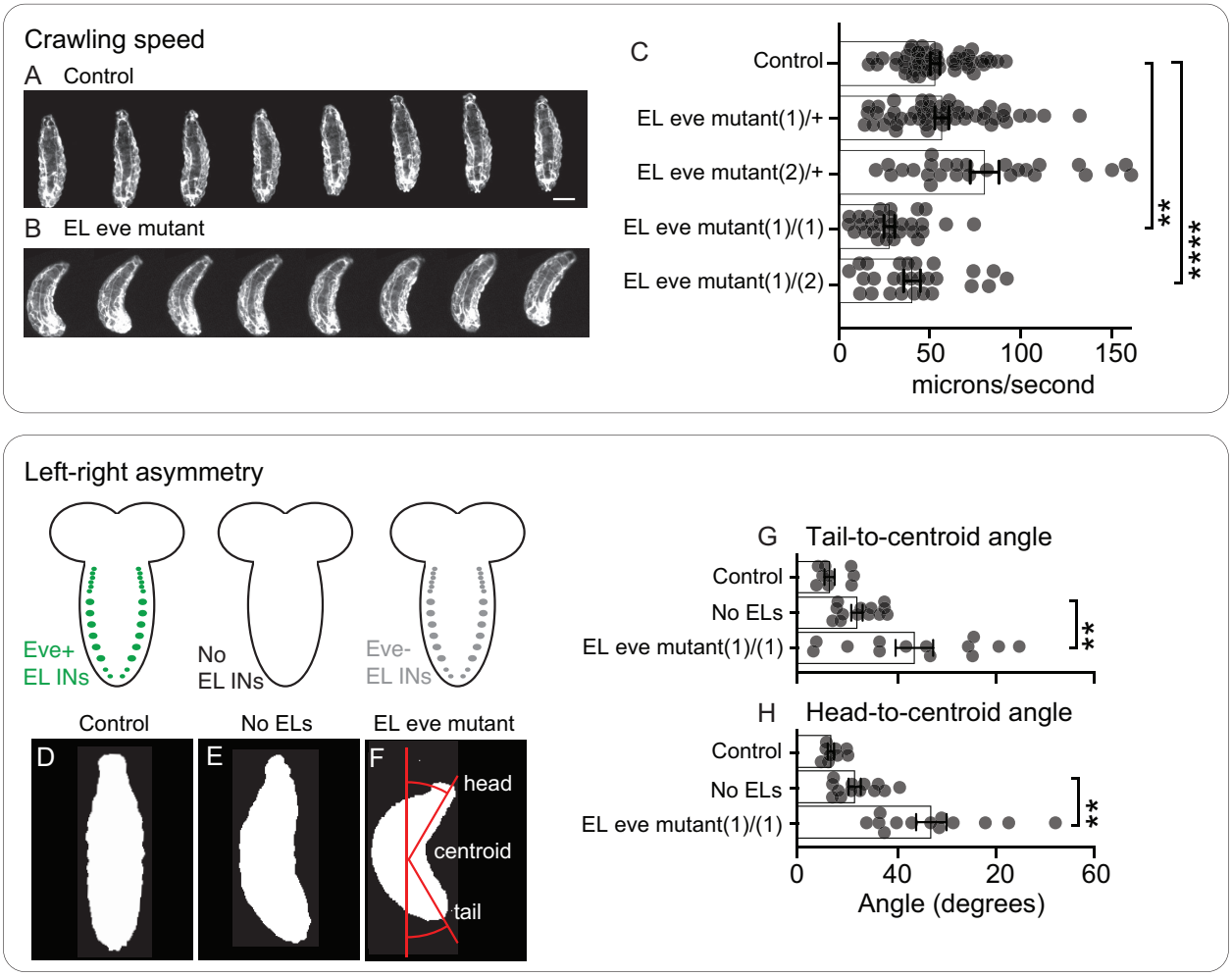

Figure 9

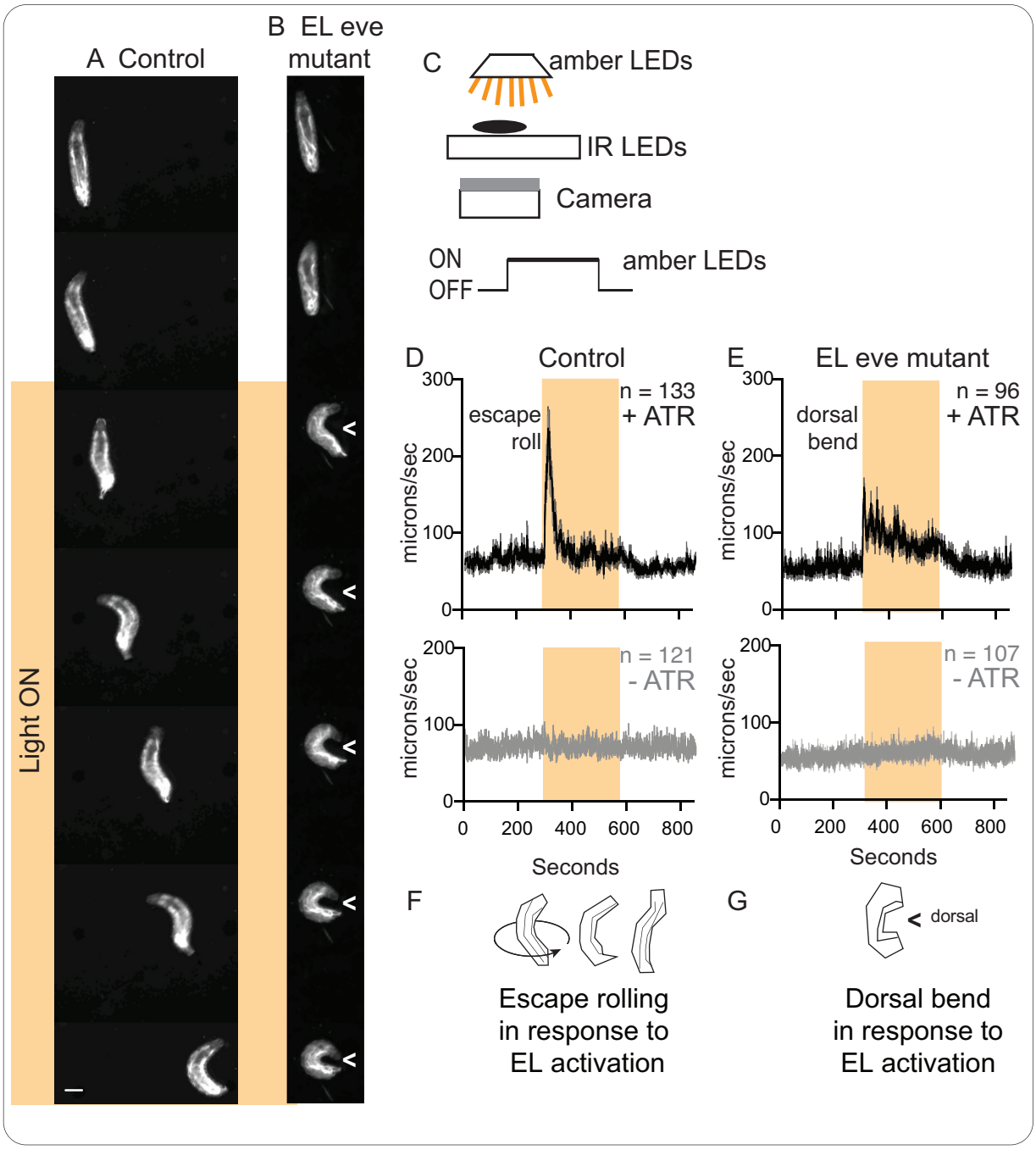

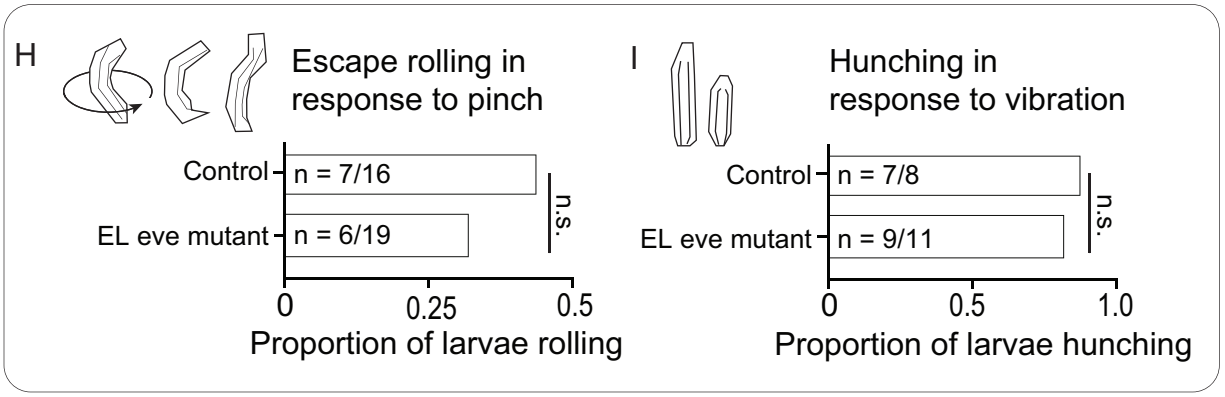

Figure 10.